

Internetworking Indonesia Journal

The Indonesian Journal of ICT and Internet Development

- Guest Editors' Introduction: Special Issue on Instrumentation,
Control and Automation 1
by Endra Joelianto & Estiyanti Ekawati
- Construction and Operation of the MARS-CT Scanner 3
*by R. Zainon, A.P.H. Butler, N. J. Cook, J. S. Butzer, N. Schleich, N. de Ruiter,
L. Tlustos, M. J. Clark, R. Heinz & P.H. Butler*
- Analysis Throughput Multi-code Multicarrier CDMA S-ALOHA 11
by Hoga Saragih
- Intelligent Learning Objects (LOs) Through Web Services Architecture 17
by Ahmad Luthfi
- Industrial Control Quality Improvement using Statistical Process Control:
Tennessee Eastman Process Simulation Case 23
by Endra Joelianto & Linda Kadarusman
- FPGA Simulation of AD Converter by using Giga Hertz Speed 29
Data Acquisition for Partial Discharge Detection
*by Emilliano, Chandan Kumar Chakrabarty, Ahmad Basri,
Agileswari K. Ramasamy & Lee Chia Ping*

Volume 2
Number 1
Spring 2010

ISSN: 1942-9703
IJ © 2010
www.InternetworkingIndonesia.org

Internetworking Indonesia Journal

The Indonesian Journal of ICT and Internet Development

ISSN: 1942-9703

Internetworking Indonesia is a semi-annual electronic journal devoted to the timely study of Information and Communication Technology (ICT) and Internet development in Indonesia. The journal seeks high-quality manuscripts on the challenges and opportunities presented by information technology and the Internet in Indonesia.

Journal mailing address: Internetworking Indonesia Journal, PO Box 397110 MIT Station, Cambridge, MA 02139, USA.

Co-Editors

Thomas Hardjono, PhD
(MIT Kerberos Consortium, MIT, USA)

Budi Rahardjo, PhD
(ITB, Indonesia)

Kuncoro Wastuwibowo, MSc
(PT. Telkom, Indonesia)

Editorial Advisory Board

Prof. Edy Tri Baskoro, PhD (ITB, Indonesia)
Mark Baugher, MA (Cisco Systems, USA)
Lakshminath Dondeti, PhD (Qualcomm, USA)
Paul England, PhD (Microsoft Research, USA)
Prof. Svein Knapskog, PhD (NTNU, Norway)
Prof. Merlyna Lim, PhD (Arizona State University, USA)

Prof. Bambang Parmanto, PhD (University of Pittsburgh, USA)
Prof. Wishnu Prasetya, PhD (Utrecht University, The Netherlands)
Graeme Proudler, PhD (HP Laboratories, UK)
Prof. Jennifer Seberry, PhD (University of Wollongong, Australia)
Prof. Willy Susilo, PhD (University of Wollongong, Australia)
Prof. David Taniar, PhD (Monash University, Australia)

Technical Editorial Board

Moch Arif Bijaksana, MSc (IT Telkom, Indonesia)
Teddy Surya Gunawan, PhD (IIUM, Malaysia)
Dwi Handoko, PhD (BPPT, Indonesia)
Mira Kartiwi, PhD (IIUM, Malaysia)
Bobby Nazief, PhD (UI, Indonesia)
Anto Satriyo Nugroho, PhD (BPPT, Indonesia)

Bernardi Pranggono, PhD (University of Leeds, UK)
Bambang Prastowo, PhD (UGM, Indonesia)
Bambang Riyanto, PhD (ITB, Indonesia)
Andriyan Bayu Suksmo, PhD (ITB, Indonesia)
Henri Uranus, PhD (UPH, Indonesia)
Setiadi Yazid, PhD (UI, Indonesia)

Manuscript Language: The Internetworking Indonesia Journal accepts and publishes papers in Bahasa Indonesia and English.

Manuscript Submission:

- Manuscripts should be submitted according to the IEEE Guide for authors, and will be refereed in the standard way.
- Manuscript pages should not exceed 7 pages of the IEEE 2-column format. It should be submitted as a Microsoft-Word file, using the IJ Template document which can be found at the www.InternetworkingIndonesia.org website.
- Manuscripts submitted to the IJ must not have been previously published or committed to another publisher under a copyright transfer agreement, and must not be under consideration by another journal.
- Papers previously published at conferences can be submitted to the IJ, but must be revised so that it has significant differences from the conference version.
- Authors of accepted papers are responsible for the Camera Ready Copy formatted using the same IJ Template format.
- Authors are advised that no revisions of the manuscript can be made after acceptance by the Editor for publication. The benefits of this procedure are many, with speed and accuracy being the most obvious.
- Please email your papers (or questions) to: editor@InternetworkingIndonesia.org

Submission Guidelines: Please review the descriptions below and identify the submission type best suited to your paper.

- *Research Papers:* Research papers report on results emanating from research projects, both theoretical and practical in nature.
- *Short papers:* Short research papers provide an introduction to new developments or advances regarding on-going work.
- *Policy Viewpoints:* Policy Viewpoints explore competing perspectives in the Indonesian policy debate that are informed by academic research.
- *Teaching Innovation:* Teaching Innovation papers explore creative uses of information technology tools and the Internet to improve learning and education in Indonesia.
- *Book Reviews:* A review of a book, or other book-length document, such as a government report or foundation report.

Guest Editors' Introduction: *Special Issue on Instrumentation, Control & Automation*

THIS special issue in the *Internetworking Indonesia Journal* (IJJ) represents the extended version of selected papers presented in the *International Conference on Instrumentation, Control and Automation* (ICA 2009) held on 20-22 October 2009 in Bandung, Indonesia. The international conference was organized by the Instrumentation and Control Research Group, Faculty of Industrial Technology, Bandung Institute of Technology (ITB). The conference is the tenth conference in the series, with the last event being the 9th Conference of Instrumentation and Control (CIC'2007) and the national Seminars on Instrumentation and Control. These were regularly hosted by the Instrumentation and Control Laboratory, Department of Engineering Physics, Faculty of Industrial Technology, Bandung Institute of Technology since 1988.

The international conference addresses the most recent topics in instrumentation, control and automation, both in research stages and industrial developments. It is the goal of the conference to become the scientific forum for academics, researchers, and practitioners, to share ideas, experiences, vision and information in this field. For over the 20 years of the running of these seminars and conferences, the group has fostered a solid community of instrumentation, control and automation in Indonesia.

In this special issue, five papers were selected to represent the investigation, the development and the application of information and communication technology in the area of instrumentation, control and automation.

The title of the first paper is the Construction and Operation of the MARS-CT Scanner. This paper presents the development of a spectroscopic CT scanner with capability of taking multiple energy CT images of small animal and pathology specimen. The researchers designed and constructed a gantry with corresponding control electronics and software to drive a conventional x-ray tube and a Medipix2 x-ray detector around an object of up to 100 mm diameter. The scanned images subsequently reconstructed into a 3D spectroscopic projection data. This study successfully takes 3D images at 43 μm resolution for small objects such as mice.

The second paper proposes the utilization of a random access scheme Slotted ALOHA (S-ALOHA) to improve the performance of multi-code multi-carrier code-division multiple accesses (MC-MC-CDMA) systems. The

improvement is demonstrated in forms of the increase of number of assigned codes and sub-carriers, higher throughput for high bit rate signal transmission.

The third paper presents the Intelligent Learning Objects (LOs) Through Web Services Architecture. The authors has identified and created common Web services, which essential for the creation and authoring stages of typical e-Learning system architecture by utilized Learning Objects (LOs). These services provide a common interface between various components leading to the platform independence, the interoperability between learning systems and the function reusability of e-Learning platform.

The fourth paper presents the improvement of industrial control quality by using a statistical process control method. The authors uses the classical Tennessee Eastman Process Simulation Case to demonstrate the advantage of using the statistical process control module to evaluate the operation cost, the product quality, process pressure, and production rate, as well as to tune the control parameters.

The fifth paper demonstrates the utilization of ISE Simulator version 9.2i (Xilinx) and the very high integrated circuit hardware description language (VHDL) programming to evaluate the use of Field Programming Gate Array (FPGA) in a circuit for the detection and counting of partial discharge signals in underground cable.

The guest editors would like to thank to Editorial Board of IJJ and especially Dr. Thomas Hardjono as the Chief Editor for his support and encouragement from preparation until finalization of the selected papers of the International Conference on Instrumentation, Control and Automation (ICA) 2009 in the *Internetworking Indonesia Journal* (IJJ). The contribution from the invited authors is gratefully acknowledged. The guest editors would like to congratulate all authors for their efforts in preparing such excellent extended papers. The editors wish that the readers will find this issue not only stimulating but also helpful and practicable in instrumentation, control and automation areas.

Endra Joelianto
Estiyanti Ekawati

The Guest Editors can be reached at the following email addresses. Dr. Endra Joelianto is at ejoel@tf.itb.ac.id, while Dr. Estiyanti Ekawati is at esti@tf.itb.ac.id.

Dr. Endra Joelianto received the B.Eng. degree in Engineering Physics from Bandung Institute of Technology, Indonesia in 1990, and Ph.D. degree in Engineering from The Australian National University (ANU), Australia in 2002. Since 1999, he has been with the Department of Engineering Physics, Bandung Institute of Technology, Bandung, Indonesia, where he is currently an Assistant Professor. His research interest includes hybrid control systems, discrete event systems, artificial intelligence, robust control, unmanned systems and intelligent automation. He has edited one book on intelligent unmanned systems published by Springer-Verlag, 2009 and published more than 70 research papers. Dr. Joelianto currently is an Editor of the International Journal of Artificial Intelligence (IJAI) and the International Journal of Engineering and Technology (IJET). He is the Chairman of Society of Automation, Control & Instrumentation, Indonesia. He was the General Chair of the International Conference on Instrumentation, Control and Automation (ICA), Bandung 2009.

Dr. Estiyanti Ekawati obtained the B.Eng. degree in Engineering Physics Department in 1992 and the M.Eng. degree in Instrumentation and Control in 1997 from Bandung Institute of Technology. She received the Ph.D. degree in Engineering in 2004 from Murdoch University, Australia. Dr. Ekawati is a lecturer at the Faculty of Industrial Technology, Bandung Institute of Technology and a research and operational manager at the Center for Instrumentation Technology and Automation (CITA) in the same university. Her research interests include the areas of mathematical programming and its application in process systems and mechanical systems engineering, also the design and implementation of industrial instrumentation and control systems.

Construction and Operation of the MARS-CT Scanner

R. Zainon¹, A.P.H. Butler², N. J. Cook³, J. S. Butzer⁴, N. Schleich⁵, N. de Ruiter⁶, L. Tlustos⁷,
M. J. Clark⁸, R. Heinz⁹ and P.H. Butler¹⁰

Abstract— The aim of this project is to build a spectroscopic CT scanner capable of taking multi energy CT images of small animal and pathology specimens. The current prototype scanner uses a conventional x-ray tube and a Medipix2 x-ray detector (developed by the European Organisation for Nuclear Research - CERN) that is capable of photon counting and energy discrimination. The scanner is referred to as the Medipix All Resolution System-CT (MARS-CT). We designed and constructed the gantry and control electronics so that the detector and x-ray tube could be rotated around an object of up to 100 mm diameter. Software was written to control the scanner and to reconstruct the spectroscopic projection data into a 3D volume, using cone beam filtered back projection. The

scanner successfully takes 3D images at 43 μm resolution. The user is able to define the energy ranges known as energy bins. The scanner's stability, accuracy and image quality was proven and tested. We successfully scanned a range of small objects including mice.

Index Terms— computed tomography, Medipix, photon counting detector, spectral x-ray imaging.

Manuscript received February 18, 2010. This work was supported by New Zealand Foundation for Research, Science, and Technology (PROJ-13860-NMTS-UOC).

¹R. Zainon is with the Department of Physics and Astronomy, University of Canterbury, Christchurch, New Zealand. She is also a fellow from Advanced Medical and Dental Institute, Science University of Malaysia, No 1-8 (Lot 8), Persiaran Seksyen 4/1, Bandar Putra Bertam, 13200 Kepala Batas, Pulau Pinang, Malaysia (e-mail: rbz10@student.canterbury.ac.nz).

²A.P.H. Butler is with Department of Radiology, University of Otago, Christchurch, New Zealand. He is also with the Department of Electrical and Computer Engineering, University of Canterbury, Christchurch, New Zealand and European Organisation for Nuclear Research (CERN), Geneva, Switzerland (e-mail: anthony@butler.co.nz).

³N. J. Cook is with the Medical Physics and Bioengineering, Canterbury District Health Board, Christchurch, New Zealand (e-mail: nick.cook@cdhb.govt.nz).

⁴J. S. Butzer was with Department of Physics and Astronomy, University of Canterbury, Christchurch, New Zealand (e-mail: jsb695@student.canterbury.ac.nz).

⁵N. Schleich is with Department of Physics and Astronomy, University of Canterbury, Christchurch, New Zealand and she is also with the Medical Physics and Bioengineering, Canterbury District Health Board, Christchurch, New Zealand (email: Nanette.Schleich@cdhb.govt.nz).

⁶N. de Ruiter is with the HIT Lab NZ, University of Canterbury, Christchurch, New Zealand (e-mail: njr47@student.canterbury.ac.nz).

⁷L. Tlustos is with the European Organisation for Nuclear Research (CERN), Geneva, Switzerland (e-mail: Lukas.Tlustos@cern.ch).

⁸M. J. Clark was with Department of Physics and Astronomy, University of Canterbury, Christchurch, New Zealand (e-mail: mjc224@student.canterbury.ac.nz).

⁹R. Heinz was with Department of Physics and Astronomy, University of Canterbury, Christchurch, New Zealand (e-mail: richardheinz@gmx.de).

¹⁰P.H. Butler is with the Department of Physics and Astronomy, University of Canterbury, Christchurch, New Zealand. He is also with the European Organisation for Nuclear Research (CERN), Geneva, Switzerland (e-mail: phil.butler@canterbury.ac.nz).

An earlier version of this paper was presented at the ICA2009 International Conference in October 2009 in Bandung, Indonesia.

I. INTRODUCTION

INTEREST in dual energy computed tomography (Dual Energy CT, or DECT) has grown in recent years following the development of commercial systems for clinical use. These systems work by having either two x-ray tubes or a single x-ray tube operated at two voltages. The aim of our work was to construct an x-ray CT scanner capable of acquiring a 3D dataset in multiple energy bins. It provides spatial and energy information at the same time so is referred to as Medipix All Resolution System CT (MARS-CT).

Spectroscopic x-ray detectors such as CERN's Medipix detectors offer the possibility of energy-selective biomedical x-ray imaging. The MARS-CT scanner is part of a new generation of CT scanners using this new type of x-ray detector. These detectors count individual x-ray photons within specified energy windows. This allows for CT images of objects to be obtained with spectral information [1]. The current prototype scanner, MARS-CT, is being operated and tested at the Bioengineering Laboratory in the Department of Radiology at Christchurch Hospital. Groups within the Medipix collaboration as well as suppliers of medical x-ray systems are working on reconstructing the material composition from radiographs [2].

II. SCANNER COMPONENTS AND OPERATION

The MARS-CT system is a desktop x-ray CT scanner consisting of a micro focus x-ray tube aligned with an x-ray detector. This is placed in a rotating gantry controlled by a motor system. It enables us to image small (up to 100 mm diameter and 200 mm length) animals and biological samples. The scanner was designed to take full advantage of the high spatial and energy resolution that Medipix2 offers (55 μm square pixels). Energy resolution is limited by detector

characteristics such as sensor material and low energy charge-sharing effects.

The scanner was built to prove both the detector's abilities and the scanner design; it had to be safe, robust, architecturally flexible, transportable and affordable. Figures 1, 2, 6, 7 and 8 show a MARS-CT scanner design, a photograph of the completed MARS-CT gantry, the object and detector translation axes, MARS-CT scanner and a top view of the loaded specimen, respectively.

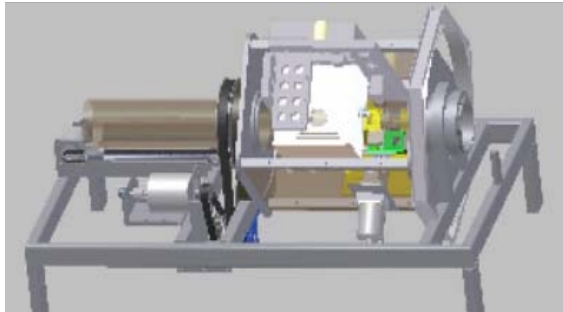


Figure 1: MARS-CT scanner design

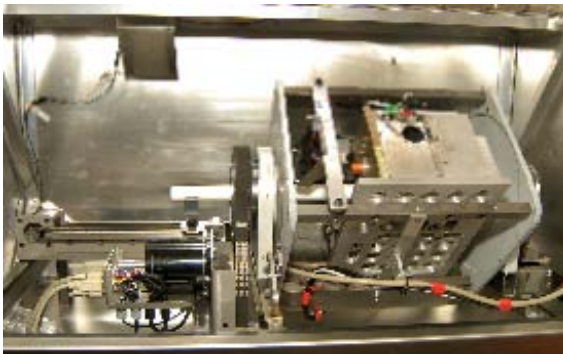


Figure 2: Completed MARS-CT gantry

In Figure 3, different types of CT imaging techniques are given. These range from standard (broad spectrum) CT to dual-energy CT and spectral CT (MARS-CT) [3]. In standard CT, machines are only capable of measuring the overall attenuation of x-rays as they pass through an object. Each material's x-ray attenuation depends on its atomic number and electron density. A CT image is created by directing x-rays through an object from multiple orientations and measuring their resultant decrease in intensity. The grey levels in a CT slice correspond to x-ray attenuation, which reflects the proportion of x-rays scattered or absorbed as they pass through each voxel. Standard single energy CT characterises tissues with a single scalar value (Hounsfield Unit) giving total attenuation in a voxel.

Dual-energy CT systems have been developed as a technique for improving material separation capabilities by using x-rays from a single source repeated at a different tube kilovoltage, or by using dual sources (x-ray tubes at 90°). While dual-energy CT obtains additional information about the elementary chemical composition of the scanned material, images are limited to two energies with overlapping x-ray spectra. In addition, rotation of the gantry or x-ray tube offset

produce spatial registration errors between each of the two energies.

Most CT advances have been to improve the use of absorption information and to reject scattering information. Of all the areas of possible improvement for radiation detectors, energy discrimination of incident x-ray photons is the most promising [4]. Energy discriminating photon counting pixel detectors, such as Medipix, enable recording of energy spectrum of the x-ray beam.

MARS-CT uses a single standard x-ray beam with a spectral detector. Thus, multiple energy measurements can be obtained. The Medipix detector is a photon counting detector. That is, it records the properties of an x-ray beam on a photon by photon basis with virtually no detector noise. In particular, each pixel of the Medipix detector has the electronics to measure and record the energy of each photon. The extra energy information provides enhanced differentiation between tissue types such as bone, muscle, fat and contrast agents without the drawbacks of the dual source approach.

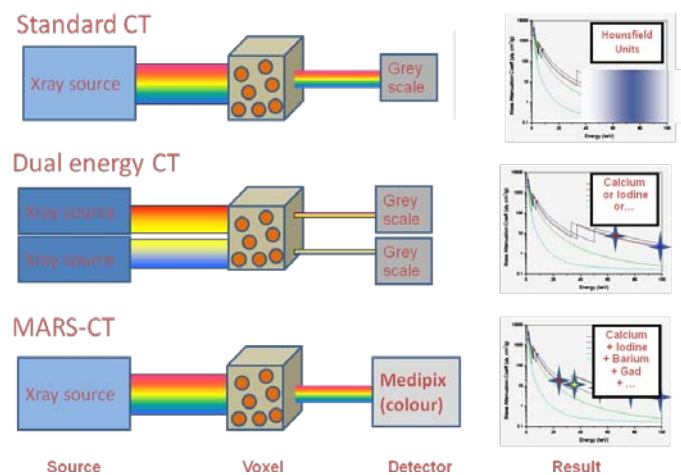


Figure 3. Different types of CT imaging techniques

A. Medipix2 Detector and the Detection Principle of x-rays

Advances in CMOS technology have opened up new possibilities in particle detection and imaging. In recent years, particle physics experiments have been transformed by the introduction of application-specific integrated circuits (ASIC) particularly for tracking detectors. Pixel detectors have become key components in tracking systems, especially in high radiation environments where excellent spatial resolution is combined with extremely high signal to noise ratios. This allows physicists to find evidence of rare particle tracks in very complicated events [5]. The Medipix2 chip demonstrated that the photon counting approach provides images with excellent dynamic range which are practically free of non-photonic noise [6]-[7]. Figure 4 shows a schematic diagram of the Medipix2 detector.

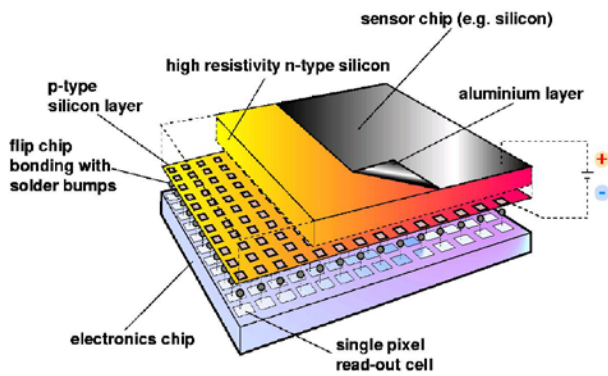


Figure 4: Schematic diagram of Medipix2

The Medipix2 chip (Figure 5) consists of 256 x 256 identical elements. Each works in single photon counting mode for positive or negative input charge signals.

An incident x-ray photon generates a cloud of electron-hole pairs in the semiconductor (eg. silicon or CdTe) sensor layer of the detector. These charge pairs are measured by the underlying ASIC layer. The electronics of each pixel counts the photons incident on the sensor, but can also be set to only count photons that fall within a certain energy range. Each Medipix2 pixel is $55 \mu\text{m}^2$, giving a spatial resolution comparable to mammographic film; the film with the smallest grain size in regular use in medical imaging. Each Medipix2 pixel acts as an individual spectral detector. The logic circuits for each pixel (approximately 600 transistors) can analyse incoming events at near megahertz rates, comparing the charge of the electron-hole cloud with preset threshold levels. That is, an incident photon is only counted if its energy is above this software selectable threshold. The results are to have an imaging detector with a spatial resolution of $55 \mu\text{m}^2$ and an energy resolution of about 2 keV across the range of 8 – 140 keV.

In summary, the Medipix2 detector is a hybrid ionising particle detector designed to provide energy selective images at high spatial and temporal resolutions. These position sensitive detectors have been successfully used in spectroscopic radiation measurements [6].

In Medipix3, the latest version of the chip, each pixel has two thresholds and two counters allowing for two simultaneous energy measurements with. In addition it has another mode in which group of four pixels communicates to produce a super-pixel capable of simultaneously reading eight energy windows simultaneously. These allowing for true spectroscopic CT without multiple x-ray exposures. Medipix3 also has significantly improved energy resolution because each pixel communicates with its neighbor to correct for charge sharing effects.



Figure 5: Medipix2 detector

B. MUROS Readout System

The Medipix2 re-Usable Readout System, version 2, (Muros2) board is an interface between a board carrying a maximum of four Medipix2 chips and a National Instruments DIO-653X board. The Muros2 has been developed at the National Institute for Nuclear Physics and High Energy Physics (NIKHEF) as a successor to the Muros1 board, (designed for Medipix1) [7]. The Muros2 board supports serial communication with the Medipix2 chip.

C. Gantry and Housing

The scanner is built around a stable steel frame made of 50 x 25 mm² welded box-section steel. This is designed to keep any twisting or vibration to a minimum. The scanner gantry is constructed from two solid steel endplates attached to each other by four steel rods to form a strong and rigid rotating unit. The endplates rotate on large diameter bearings, leaving a 106 mm hole for sample tubes to pass through. This gives a maximum sample size of 100 mm. One side of the gantry is formed by a solid steel base plate, which provides support for the x-ray tube and the detector. All sides are covered by stainless steel panels, one of which has a primary 3 mm lead barrier for radiation shielding.

The scanner is housed in a lead shielded box (Figure 5) which consists of 1.8 mm lead sandwiched between 0.5 mm aluminium and 0.5 mm stainless steel. The box has interlocked access on sample doors, and shielded ports for cable entry and ventilation. A warning light on the scanner box is illuminated when x-rays are being produced. There is no measurable radiation outside the box. Cables going to the rotating gantry are arranged to accommodate a half twist as they leave the scanner through a port in line with the centre of rotation.

The micro focus tube and high voltage generator are fixed to a base plate on one side of the gantry. This base plate can be moved in or out to give the most efficient position ensuring complete coverage of the sample object. A fan has been mounted to cool the x-ray tube and allow continuous operation at full current. On the opposing side, a Medipix2 detector is positioned. It is mounted on a plate that allows fine angular adjustment to ensure the detector pixels are aligned with the vertical axis. Since the detectors are small (either a

single detector chip at $14 \times 14 \text{ mm}^2$ or a quad detector assembly at $28 \times 28 \text{ mm}^2$) they may need to be translated vertically to create a complete projection radiograph. The mounting plate is connected to a screw drive which accurately translates the detector to each imaging position. The screw drive is supported by the steel base plate and can be translated perpendicular to the access of rotation to accommodate different sample sizes, which range from 25 to 80 mm.

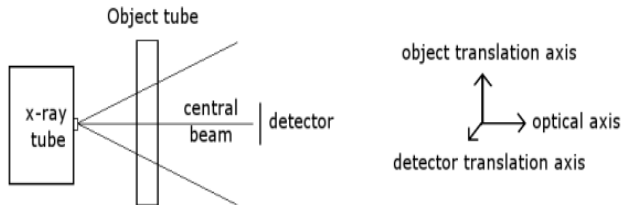


Figure 6: The scanner axes

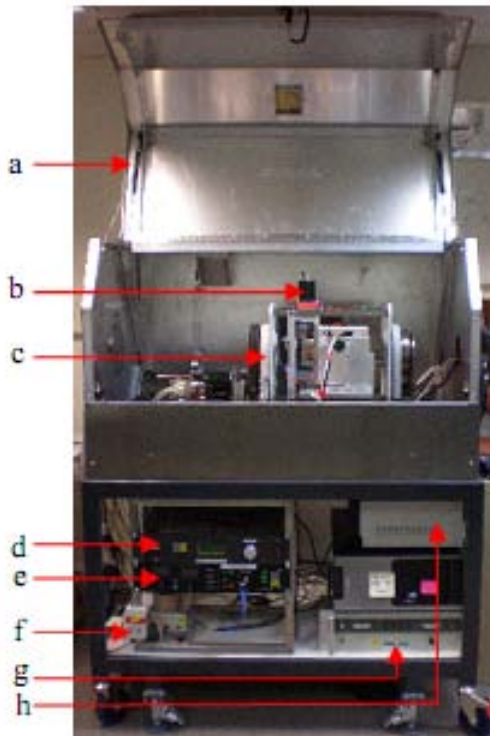


Figure 7: MARS-CT scanner with its main components labelled (a) lead shielded box, (b) stepper motor, (c) gantry, (d) motor controller, (e) x-ray controller, (f) fan switch, (g) power supply and (h) MUROS power.

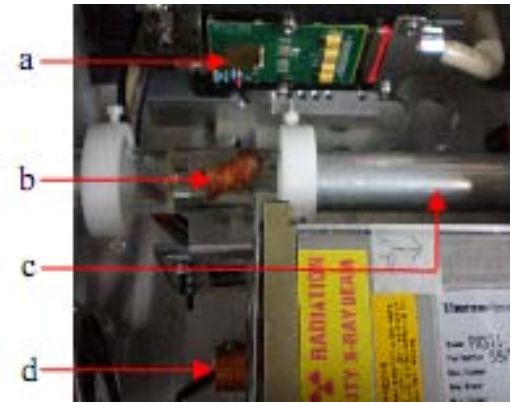


Figure 8: The MARS-CT gantry with its main components labelled (a) Medipix2 detector, (b) sample (in this case a human atheroma plaque fixed in Perspex), (c) sample holder and (d) micro focus x-ray tube.

D. X-ray tube

A Thermo Scientific Kevex PXS11-150-75 is the x-ray source for the MARS-CT scanner. It is a portable x-ray source with 75 kV and 11.25 W. It has constant potential and mini-focus for use in high resolution radiography and real time imaging applications. The $40 \mu\text{m}$ spot size delivers high resolution direct x-ray magnified images over the entire range of operation. In spite of its high performance, the Kevex PXS11 uses a filament cathode, thereby eliminating the need for bias or focus supplies which are necessary for dispenser cathode type x-ray tubes.

The Kevex PXS11 combines the x-ray tube, high voltage power supply and control circuitry in one compact package that is powered from a 28 VDC source. The specifications of this micro focus x-ray tube include: a 8.9 mm Focus-to-Object Distance (FOD) which enables high magnification; a high flux output of 70 R/min at 11.25 W; an operating voltage range of $40\text{--}75 \text{ kV} \pm 1\%$, which enables use with a wide range of materials; an integrated source-tube power supply and control circuitry; an internal cooling fan. The x-ray tube weight is approximately 4 kg.

E. Operation of the MARS-CT scanner using Medipix2

The operation of the x-ray tube, the stepper motors and the Medipix2 detector is controlled by Matlab on a dedicated PC. Serial interfaces are used for the x-ray tube and stepper motors. The Medipix2 detector is read using Pixelman software [8] via a custom designed Pixelman-Matlab interface. The user defines a number of parameters before scanning. These include the number of rotational steps, the number of sensor positions (to enlarge the field of view), the threshold settings and corresponding acquisition times. In order to simplify cable management on the gantry, the scanner is designed to complete one revolution and then return to the starting position.

The detector and x-ray source are mounted on the gantry with the sample between. An image (called a frame) is taken and then gantry rotated. Then the detector and source are rotated around the sample. At the next stop another next

projection frame is taken. This process is repeated around the entire sample. The number of stops and therefore projection frames taken is determined by the user. For larger samples the detector can be moved linearly up and/or down and the process repeated. This creates more than one frame at each rotation stop. The frames are stitched together to form the projection images. A small overlap of a few pixels maintained in the movement to help check alignment and to ensure consistent exposures. All scanner control and image triggering is performed via Matlab routines. Table 1 shows an example of typical scan parameters for four energy bins. The reduced time at lower energies is to ensure that a similar number of photons are measured above each threshold.

Table 1: Scan parameters for mouse with four energy bins

Energy (keV) of the low threshold	12	17	33	42
Time (s)	0.3	0.3	1.5	3.0

III. IMAGE RECOVERY, PROCESSING AND VISUALISATION

Images obtained from the multi-energy MARS-CT scanner were processed by back projection to a 3D volume data set using Octopus version 8.2 [9]. Octopus is commercial tomography reconstruction software for cone beam CT, spiral CT, or parallel beam CT. The software allows the user to change a number of settings concerning the pre-processing and filtering. Pre-processing steps are included in the package such as ring filtering, normalisation, beam hardening correction and axis tilt correction.

In addition, the CBCT reconstruction algorithm was also implemented in Matlab to reconstruct images from the projections. A variation of the Feldkamp, Davis and Kress cone-beam computed tomography (CBCT) algorithm (T-FDK-algorithm) [10] was used to reconstruct the images. This includes two steps of rebinning the projection data and performing a filtered backprojection. Additional pre-processing of the raw projection data was required due to the special scanner geometry.

The point source emits a cone shaped beam, which is detected by the two-dimensional Medipix detector. The detector rotates simultaneously around the centre of rotation, which ideally is in the centre of the object. Each pixel of the projections obtained with a cone-beam can be characterized by the rotation angle α , the fan angle γ and the cone angle θ . In the first step of rebinning, the so called row-wise rebinning, one row of the pixels is taken which implies a fixed value of the cone angle θ . The lot of the same rows from all projections represents a fan-beam set-up and can be converted into parallel-beam geometry. Each set of rotation angle and fan angle can be described by a corresponding pair of rotation angle and distance u of the x-ray detected by this specific pixel to the centre of rotation.

Now using one column of this row-wise rebinned data at a time (fixed value of u), the second step of rebinning is done which involves projecting the row-wise rebinned data onto a planar and rectangular virtual detector. After applying a weighting factor to each pixel accounting for the angle of the

x-ray detected by this specific pixel to the horizontal plane, the object can be reconstructed with filtered backprojection.

The 3D reconstructed images can be used for visualisation purposes to produce a more comprehensive model of the object. A research program for volumetric visualisation, called MARSExplorer, is being developed for the interactive exploration of the spectroscopic data as volumetric objects. This will allow for better diagnosis and interpretation of medical and biological data. MARSExplorer provides multiple views to allow for comparison of energy bins side by side or multiple views of the same energy bin. Each view can combine energy bins with simple techniques including finding the average, difference, and maximum and minimum voxels between two energy bins. Also, three energy bins can be assigned to the three primary colours to directly compare brightness levels of the voxels and contrast the differences with the resulting colour (colour combination mode).

MARSExplorer provides a basic set of volumetric tools for navigating through the energy bins. These tools include slicing the volume, controlling the transparency and thresholding the luminance range. The tools are mapped to slider bars to allow for fast and interactive control over the volume. The algorithm for direct volumetric rendering is based on the volume rendering integral. Furthermore, a Maximum Intensity Projection algorithm and an iso-surface algorithm are integrated into MARSExplorer. Also included is a volumetric PACS viewer, which allows the direct view of any slice of the energy bin in any orientation.

The performance of MARSExplorer is dependent on the hardware of the desktop PC. With a PC containing a GeForce 8800 GT graphics card with 512Mb video RAM, up to 1800 slices of 512 x 512 pixels (16 bit, tiff images) can be stored on the graphics card. The frame rate peaks at 60fps depending on the number of iterations chosen, for the volume rendering integral. The standard settings for direct volume rendering with four views results are 30 fps.

The tools for navigating through the volumes include slicing, transparency, threshold and iteration controls as well as pan, rotate and scale tools. Most of these tools are currently mapped to the keyboard, but widgets are being developed so that the program interface is more interactive, for example the slider bars which control the slicing. While artefacts are still visible the volume is clear. Continual improvements are being made to the program moving it from its basic form to incorporate more complex rendering algorithms. An additional program called osgMARSImage was created for 3D visualisation of the scanned objects.

IV. RESULTS AND DISCUSSION

To date several objects have been scanned. These include test phantoms and mice. We were able to successfully obtain multi-energy CT images with a spatial resolution of 43 μ m. Example images are shown in Figures 9, 10 and 11. The cross section of a mouse abdomen, volume rendering of a mouse skull and paws and 3D image of the mouse respectively, are

shown.

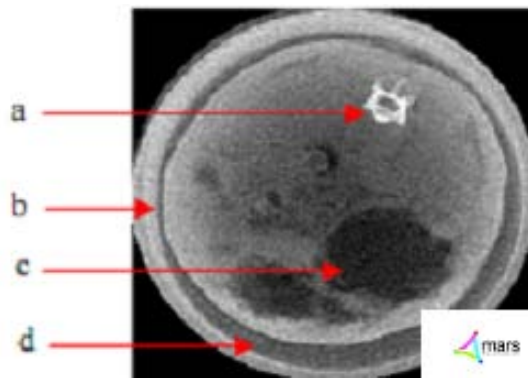


Figure 9: Cross section of a mouse abdomen with its main components labelled (a) spine, (b) support tube, (c) stomach and (d) air.

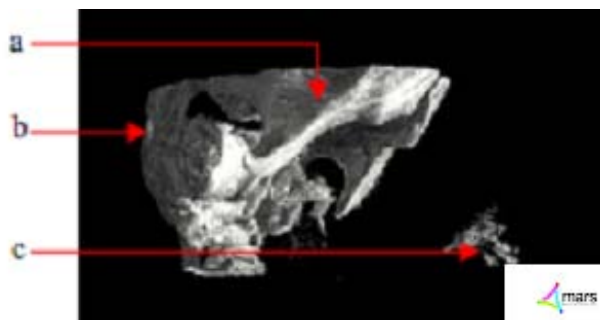


Figure 10: Volume rendering of a mouse with its main components labelled (a) jaw, (b) skull base and (c) paws.

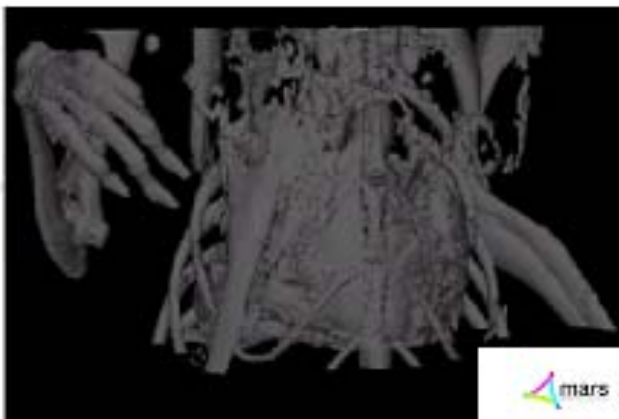


Figure 11: 3D image of a mouse

Besides these advantages of CT many further important clinical applications had been discovered by our spectroscopic CT and provide valuable findings in medical imaging. We had shown that MARS-CT scanner has the potential in atherosclerotic plaque imaging [11]-[12]. Currently, dual-energy CT has led the discrimination between different tissue types in atherosclerotic plaque. Results from dual-energy CT suggests that spectra CT is feasible for the discrimination of iron and calcium, both of which may be of similar attenuation on single energy CT images. Identification of iron and calcium plaque components might allow for the non-invasive

detection of unstable plaque *in vivo*.

Moreover, we are able to improve evaluation of non-alcoholic fatty liver disease (NAFLD) using novel spectroscopic-CT scanner to improve the. NAFLD has become the most common form of liver disease in Western communities, affecting an estimated 17-33% of American adults [13]. Primary NAFLD is the liver component of the “metabolic syndrome”, a collection of diseases associated with obesity [14]. The clinical spectrum of NAFLD ranges from simple fatty liver or steatosis, to non-alcoholic steatohepatitis (NASH, fatty liver with inflammation and evidence of hepatocyte damage), cirrhosis, and hepatocellular carcinoma or liver failure [13]. In addition, x-ray attenuation curves (mass attenuation curves) have been measured for a variety of elements, compounds and mixtures, including adipose tissue, and are well understood [15].

Mass attenuation curves are traditionally measured on a spectroscope, by scanning a monochromatic X-ray beam from a monochromator through a range of energies and measuring the absorption across that range. However, unless an expensive synchrotron x-ray source is used, the beams are not intense enough to provide the spatial information required for biological imaging. We had demonstrated a method for measuring the attenuation curves of liver and fat tissue on a MARS-CT scanner with the anatomical resolution of a typical small animal microCT and with anticipated practical applications towards the quantification of fat in the liver [16].

In addition, energy resolving capabilities of x-ray detectors like the Medipix2 offer access to spectral information. This is a new domain of information for medical imaging. A conventional CT measures the cumulative attenuation of all the materials involved, a contrast agent cannot be distinguished from bone or calcifications [17]. Using Medipix technology only single x-ray source energy is needed, but the energy bins of the Medipix detector are programmed to optimally detect K-edge and slope differences between contrast agents and background tissue [18]. Identification of multiple contrast agents has already been demonstrated [19]. We have also developed a method to enhance the spectral images in the energy domain to identify the number of independent patterns of spectral variation. Principal Component Analysis (PCA) was used to identify the number independent attenuation profiles within the data [19]-[20].

V. CONCLUSION

Combining the broad energy spectrum of an x-ray tube with an energy resolving detector enables us to acquire data in chosen energy bins. This approach is different to that of dual-energy-CT, where two tubes or a modification of the energy spectrum of a single tube is used. Key benefits of MARS-CT over dual-energy systems are the use of a single x-ray tube and projection data with no overlapping energies. These are consequences of the ability of the Medipix family of detectors being able to resolve the energy of each incident photon. The

user can specify the energy windows. The energy windows can be optimised for imaging specific materials.

FUTURE WORK

The MARS-CT scanner is able to provide 3D spectroscopic x-ray images of small animals and of pathology specimens. Image processing and display techniques are being developed for best utilising this novel energy information. A variety of clinical applications have been investigated, and further experiments will be carried out using pathology specimens and mouse models of diseases. In particular, we are concentrating on applications in vascular and breast cancer imaging. Work on spectroscopic material reconstruction is ongoing. The anticipated benefits from using spectroscopic pixel detectors for medical imaging include reduction of image artefacts, better contrast imaging and improved soft tissue contrast. Initial work with the Medipix2 detector found that it is reliable and easy to use. MARS-CT is designed to incorporate future versions of Medipix, such as Medipix3 which has better energy resolution and up to eight simultaneous thresholds.

ACKNOWLEDGMENT

We would like to thank the Medipix2 and Medipix3 collaborations, NIKHEF for supplying the MUROS, Czech Technical University in Prague and Dave van Leeuwen for assisting with the Pixelman-Matlab interface.

REFERENCES

- [1] A.P.H. Butler, N.G. Anderson, R. Tipples, N. Cook, R.Watts, J. Meyer, A.J. Bell, T.R. Melzer and P.H. Butler, "Bio-medical x-ray imaging with spectroscopic pixel detectors", *Nuclear Instruments and Methods in Physics Research*, 591 (1), pp. 141-146, 2008.
- [2] M. Firsching, Jurgen Giersch, Daniel Niederlhner and Gisela Anton, "A Method for Stoichiometric Material Reconstruction with Spectroscopic x-ray Pixel Detectors", in *Proc. IEEE Nuclear Science Symposium Conference Record*, Rome, 2004, pp. 4116-4119.
- [3] N.G. Anderson, A.P.H. Butler, N. Scott, N.J. Cook, J.S. Butzer, N. Schleich, M. Firsching and P.H. Butler, "Colour CT x-ray spectroscopic images of mice using Medipix-2 detector", *European Radiology*, to be published.
- [4] G. Wang, H. Yu and De Man B., "An outlook on x-ray CT research and development", *Med Phys.*, 35(3), pp. 1051-64, 2008.
- [5] D. Di Bari et al., "Performance of 0.5×10^6 sensitive elements pixel telescope in the WA97 heavy ion experiment at CERN", *Nuclear Instruments and Methods in Physics Research*, 395 (3), pp. 391-397, 1997.
- [6] C. Schwarz, M. Campbell, R. Goeppert, J. Ludwig, B. Mikulec, K. Runge, KM Smith and W. Snoeys "Measurements with Si and GaAs pixel detectors bonded to photon counting readout chips", *Nuclear Instruments and Methods in Physics Research*, 466 (1), pp. 87-94, 2001.
- [7] B. Mikulec, "Single Photon Detection with Semiconductor Pixel Arrays for Medical Imaging Applications", PhD Thesis, University of Vienna, Austria, 2000.
- [8] T. Holy, J. Jakubek, S. Pospisil, J. Uher, D. Vavrik and Z. Vykydal, "Data acquisition and processing software package for Medipix2", *Nucl. Instrum. Meth. A* (563), pp. 254-258, 2006, doi:10.1016/j.nima.2006.01.122., (to be published).
- [9] Octopus version 8.2, CT reconstruction softwar. [Online]. Available: <http://ssf.ugent.be/linac/XRayLAB/News.html>
- [10] M. Grass, T. Kohler and Proksa, R., "3D cone-beam CT reconstruction for circular trajectories", *Physics in Medicine and Biology*, (45), pp. 329-347, 2000.
- [11] R. Zainon, S. Dufreneix, Niels de Ruitter, N.Cook, Mike Hurrell, S.P. Gieseg, A.P.H. Butler and P.H. Butler. "Spectroscopic x-ray computed tomography imaging of plaque and arteries using the Medipix detector", in *Proc. New Zealand Institute of Physics Conference*, New Zealand, 2009.
- [12] S.P. Gieseg, R. Zainon, J. Roake, A.P. Butler and P.H. Butler. "High resolution multi-energy CT imaging of atherosclerotic plaque: The future of x-ray CT imaging", in *Proc.35th Annual Scientific Meeting of the Australian Atherosclerosis Society*. Australia. 2009.
- [13] G. Farrell and C. Larter. "Nonalcoholic fatty liver disease: from steatosis to cirrhosis", *Hepatology*, 43(2), pp. 99-112, 2006.
- [14] Chandana G. Lall, Alex M. Aisen, Navin Bansal and Kumaresan Sandrasegaran. "Nonalcoholic Fatty Liver Disease", *AJR*, 190, pp. 993-1002, 2008.
- [15] J.H. Hubbell and S.M. Seltzer (1996, May). "Tables of X-Ray Mass Attenuation Coefficients and Mass-Energy Absorption Coefficients" in *Physical Reference Data*. NIST Standard Reference Database 126. [Online]. Available: <http://physics.nist.gov/PhysRefData/XrayMassCoef/cover.html>.
- [16] K.B. Berg, J.M. Carr, M.J. Clark, N.J. Cook, N.G. Anderson, N.J. Scott, A.P.M Butler, P.H. Butler and A.P.H. Butler. "Pilot study to confirm that fat and liver can be distinguished by spectroscopic tissue response on a Medipix-All-Resolution-System-CT (MARS-CT)", in *Proc. International Conference (Advanced Materials and Nanotechnology-4)*, American Institute of Physics Conference 1151, pp. 106-110, 2009.
- [17] M. Firsching, A. P. H. Butler, N. J. Scott, N. G. Anderson, T. Michel, and G. Anton. "Contrast agent recognition in small animal CT using the Medipix2 detector", *Nuclear Instruments and Methods in Physics Research Section A: Accelerators, Spectrometers, Detectors and Associated Equipment*, 607(1), pp. 179-182, 2009.
- [18] A. P. H. Butler, N. G. Anderson, M. A. Hurrell, N. J. Cook, N. J. Scott, M. Campbell and P. H. Butler. "Multiple contrast agent imaging using MARS-CT, a spectroscopic (multi-energy) photon counting microCT scanner", in *Proc. 95th Scientific Assembly and Annual Meeting of the Radiological Society of North America*, 2009.
- [19] A.P.H Butler, N. J. Cook, N. Schleich, J. Butzer, P. Bones, N.G. Anderson and P.H. Butler. "Processing of Spectral X-ray Data Using Principal Components Analysis", in *Proc.11th iWORId Conference*, Prague, Czech Republic, 2009.
- [20] J.S. Butzer, "MARS-CT: Biomedical spectral x-ray imaging with Medipix", M.Sc Thesis, Department of Physics and Astronomy, University of Canterbury, New Zealand, 2009.

Rafidah Zainon was born on 16th June 1985 in Pulau Pinang, Malaysia. She received B.Sc. (Honours) in Medical Physics from Science University of Malaysia (Universiti Sains Malaysia, USM) in 2007, M.Sc. (Medical Physics) from Science University of Malaysia (USM) in 2008 and currently pursuing Ph.D (Medical Physics) at University of Canterbury, New Zealand (commenced 2009).

She became a Trainee at Radiology Department, Science University of Malaysia Hospital, Kelantan, Malaysia in 2006, an Invigilator of International Atomic Energy Agency (IAEA) Postgraduate Educational Course (PGEC) in Radiation Protection and Safety of Radiation Sources in 2006-2007, Course facilitator in SPSS Beginner Course (with hands-on application) at School of Physics, Science University of Malaysia in 2008 and a trainee at Nuclear Medicine Department, Putrajaya Hospital and Wijaya International Medical Centre (WIMC) Hospital, Petaling Jaya, Malaysia in 2008. Currently, she is a fellow from Advanced Medical and Dental Institute, Science University of Malaysia. Her research interest is in medical imaging and currently focusing in the area of assessment of atherosclerotic plaque components with spectral CT using photon counting x-ray detector (Medipix detector).

Ms. Zainon was awarded Dean's List in 2006/2007 academic year at Science University of Malaysia (USM) and currently she was awarded scholarships from Ministry of Higher Education, Malaysia and Science University of Malaysia for USM Academic Staff Training Scheme (ASTS).

Anthony P.H. Butler was born on 25th May 1975 in Christchurch New Zealand. He received a M.B.Ch.B. (Medicine) from University of Otago, New Zealand in 1998, his F.R.A.N.Z.C.R. (Radiology) from The Royal Australian and New Zealand College of Radiologists in 2005, a Grad.Dip.Sc. (Physics) from University of Canterbury, New Zealand in 2006, and a Ph.D degree in

Electrical and Computer Engineering from University of Canterbury, New Zealand in 2007.

His current appointments are: Senior Lecturer in Radiology and Director of the Centre for Bioengineering, University of Otago Christchurch; Consultant Radiologists Christchurch Public hospital; Research Engineer in Electrical and Computer Engineering at University of Canterbury; member of both the Medipix and CMS collaborations at the European Centre for Nuclear Research (CERN). He had published more than 20 scientific papers and peer reviewed conference proceedings.

Dr. Butler has won 10 awards for his research including awards from the Royal Society of New Zealand and the Royal Australian College of Radiologists. He is a named investigator on over \$6m of New Zealand government research grants.

Philip H. Butler was born on 17th September 1947. He received B.Sc.(Hons) in Physics from University of Canterbury, New Zealand in 1967, and a Ph.D in Physics from University of Canterbury in 1970.

His current appointments are as a Professor at Department of Physics and Astronomy, University of Canterbury, Director and CEO of MARS Bioimaging Ltd and Director of Medical Laser Developments Ltd, and member of both the Medipix and CMS collaborations at the European Centre for Nuclear Research (CERN). He was Pro-Vice-Chancellor (Resources & Services) at University of Canterbury in 1998-2001, Head of Department at University of Canterbury, in 1997-1998 and 2001-2006, President of Canterbury Branch Royal Society in 1991, Fellow of New Zealand Institute of Physics in 1990. He has been a trustee of the Christchurch Science–Technology Centre Trust, (Science Alive!) since 1990, and a trustee of the National Science Technology Road show Trust since 1992.

Prof. Butler's research interests are in Mathematical Physics, especially as applied to quantum mechanics and to medical physics research and physics education. He had published more than 130 scientific papers and peer reviewed conference proceedings and 1 patents.

Analysis Throughput Multi-code Multicarrier CDMA S-ALOHA

Hoga Saragih¹
Bina Nusantara University
Jakarta, Indonesia

Abstract— This paper proposes an integrated system consisting of multi-code multicarrier code-division multiple accesses (MC-MC-CDMA) with random access scheme Slotted ALOHA (S-ALOHA), named multi-code multicarrier CDMA S-ALOHA, respectively. The performance analysis of both systems is stated as throughput. Multi-code multicarrier CDMA S-ALOHA is proposed to improve performance of multi-code CDMA or multicarrier CDMA.

In multi-code multicarrier CDMA S-ALOHA, each user is allowed to transmit multiple orthogonal codes, so the proposed MC-MC-CDMA S-ALOHA system can support various data rates, as required by the next generation standard. In MC-MC-CDMA S-ALOHA the initial data is serial to parallel converted to a number of lower rate data streams. Each stream which consists of part of the initial data called sub-packet will be coded to a number of multiple orthogonal codes then modulated using specific spreading code for each user, and all sub stream signal are transmitted in parallel on different sub carrier.

The combination of a multi-code scheme and a multi-carrier code division multiple access (MC-CDMA) and ALOHA, called MC-MC-CDMA S-ALOHA, with dual medium, is proposed and analyzed in an AWGN channel. Each medium has different characteristics in data rate transmission. The high-rate bit transmitted data user is serial to parallel converted into low-rate bit streams and assigned with multiple-orthogonal code. Each low-rate bit stream is transmitted over L orthogonal sub-carrier.

In this paper we divide interference into different types depending on codes and sub-carriers in this system, and we carry out our analysis to obtain the BER and throughput taking into account all these types.

The performance of the system is improved as the number of assigned codes and sub-carriers increases, and also the results show that the proposed MC-MC-CDMA S-ALOHA system outperforms both multi-carrier CDMA S-ALOHA and multi-code CDMA S-ALOHA in fixed bandwidth allocation.

The results show that both systems have higher throughput for high bit rate signal transmission than multi-code CDMA S-ALOHA or multicarrier CDMA S-ALOHA. It is also shown that the throughput of both systems improve as the number of code and sub carriers, while the increase of sub packet length degrades the throughput of both systems.

Index Terms : *Multiple-access protocols, CDMA, S-ALOHA, Multicode Multicarrier CDMA S-ALOHA.*

¹Hoga Saragih is with the Faculty of Computer Studies, Bina Nusantara University. An earlier version of this paper was presented at the ICA2009 International Conference in Bandung, Indonesia.

I. INTRODUCTION

Future wireless system such as third generation (3G) or fourth generation (4G) will need to flexibly provide subscribers with a variety of services such as voice, data, images, and video. Because these services have widely differing data rates and traffic profiles, future generation systems will have to accommodate a wide variety of data rates such as low-data rate or high-data rate (multi-rate).

There are two general schemes that are used to accommodate the multi-rate system Code Division Multiple Access (CDMA), namely the variable spreading gain (VSG) system scheme and the multi-code CDMA scheme [1]. The VSG system provides a variety of spreading gain for every user. The disadvantage of this system is that the spreading gain falls very low [2]. The CDMA multi-code system is able to accommodate variable data rates which is provided by multiple-code and different capacity for each of user. In a multi-code system, the spreading factor continuously keeps constant. The disadvantage of this system is that the increase of the data rate of every user will influence the increase of interference because the carrier used to transmit the signal is the same (single-carrier) [3].

CDMA systems have some disadvantages such as inter-symbol interference (ISI) and inter-chip interference (ICI) [4]. The multicarrier CDMA scheme (MC-CDMA) is one approach used to overcome those problems. Essam A. Sourour and his colleagues have researched the performance of multicarrier CDMA systems [4]. Every data user goes through a serial-to-parallel converter and then divided into low-rate data stream or low rate data symbol. Every low rate data symbol will be transmitted by some subcarrier that have narrowband bandwidth [5,6]. In [10], the BER system multi carrier DS-SS-CDMA and multirate traffic have been researched and analyzed.

The integrated system consisting of multi-code CDMA and multicarrier CDMA called multi-code multicarrier CDMA (MC-MC-CDMA) has been widely researched [1,3]. In [1], research was directed towards the performance of MC-MC-CDMA system for uplink communications. The work of [3] researched and analyzed the performance of MC-MC CDMA in single medium. The results shows that MC-MC CDMA system is better than multicarrier CDMA system and multi-code CDMA system in a certain bandwidth allocation.

This paper proposes an integrated system consisting of multi-code CDMA and multicarrier CDMA, and additionally ALOHA for dual medium traffic or dual-rate traffic. In MC-

MC CDMA ALOHA system, every user from all media will be transmitted in multiple-code through some subcarrier according to its data rate. The different characteristics of every media will influence the interference increase because of the code and subcarrier from users in the same medium and also the code and subcarrier from users in another medium.

The analyzed parameter is the throughput of MC-MC-CDMA ALOHA with dual medium or dual rate traffic in AWGN channel. The assumed system has two mediums that have different traffic profiles. The first user in medium s focused on code to- m and subcarrier to- l is a reference. The calculation of throughput is based on the consideration of the interference influencing from code and subcarrier in the same medium and also code and subcarrier in a different medium. The system also assumed that inter subcarrier and code from user is orthogonal.

The model of the system MC-MC-CDMA is explained in section 2. The explanation of BER is given in section 3 while section 4 discusses interference. Section 5 discusses MC-MC CDMA ALOHA, while section 6 presents the results and analysis of the calculation of the throughput with the results shown graphically. The conclusions are provided in section 7.

II. SYSTEM MODEL

The transmitted signal from user to- k and medium s is

$$s_k^{(s)}(t) = \sum_{m=1}^{M_s} \sum_{l=1}^L \sqrt{2P_k^{(s)}} b_{k,m,l}^{(s)}(t) c_{k,m}^{(s)}(t) \cos(\omega_l t + \theta_{k,l}^{(s)}) \quad (1)$$

From equation (1), $P_k^{(s)}$ is transmission power from user to- k and medium s , $c_{k,m}^{(s)}$ is code to- m from user k , ω_l is subcarrier frequency to- l that have initial phase $\theta_{k,l}^{(s)}$, l is the number of subcarrier in a system ($l = 1, 2, 3, \dots, L$), M_s is the number of sequence code that used in medium s , $b_{k,m,l}^{(s)}$ is transmitted data in medium s that reference in code to- m and subcarrier to- l .

$$b_{k,m,l}^{(s)}(t) = \sum_{j=-\infty}^{\infty} b_{k,m,l,j}^{(s)} h(t - jT_s) \quad (2)$$

$$c_{k,m}^{(s)}(t) = \sum_{j=-\infty}^{\infty} c_{k,m,j}^{(s)} h(t - jT_c) \quad (3)$$

$b_{k,m,l,j}^{(s)} \in \{+1, -1\}$ dan $c_{k,m,j}^{(s)} \in \{+1, -1\}$. $h(t)$ is periodic rectangular pulse with duration T_c and T_s . $h(t)$ will be 1 if $0 \leq t \leq T_s$ and will be 0 if $0 > t > T_s$. Frequency equation is orthogonality :

$$\omega_l = \omega_1 + (l-1) \frac{2\pi}{T_c} \quad (4)$$

When assume the transmission bandwidth is pass-band null-to-null $2/T_{c,l}$ and when G_{s1} is processing gain for single-code single-carrier DS-SSMA

$$G_{s1} = \frac{T_b}{T_{c1}} \quad (5)$$

Spreading code duration and processing gain for multicode multicarrier are

$$T_c = \frac{M_s L + 1}{2} T_{c1}, \text{ and} \quad (6)$$

$$G_s = \frac{M_s L T_b}{T_c} = \frac{L T_m}{T_c} = \frac{T_s}{T_c} \quad (7)$$

Substitute T_{c1} from (6) to equation (5) hence :

$$T_b = \frac{2T_c}{M_s L + 1} G_{s1} \quad (8)$$

Substitute T_b from (8) to equation (7) so that processing gain for multi-code multicarrier CDMA system is

$$G_s = \frac{T_s}{T_c} = \frac{2M_s L}{M_s L + 1} G_{s1} \quad (9)$$

Received signal is

$$r(t) = n(t) + \sum_{i=1}^S \sum_{k=1}^{K_s} \sum_{m=1}^{M_s} \sum_{l=1}^L \sqrt{2P_s} b_{k,m,l}^{(s)}(t - \tau_k^{(s)}) \times c_{k,m}^{(s)}(t - \tau_k^{(s)}) \cos(\omega_l t + \phi_{k,l}^{(s)}) \quad (10)$$

where $\phi_{k,l}^{(s)} = \theta_{k,l}^{(s)} - \omega_l \tau_k^{(s)}$, P_s is received power and assumed for all user is in the same medium. ($s = 1, 2, \dots, S$). Assumed perfect power control for every medium. For example, P_1 is received power from medium 1 and P_2 is received power from medium 2, but P_1 is not same as P_2 . $\phi_{k,l}^{(s)}(t)$ is the different between $\theta_{k,l}$ and phase that caused by time delay.

$\tau_k^{(s)}$ is time delay for user k from medium s .

III. BER APPROXIMATION

Standard Gaussian Approximation (SGA) is used, so that Multiple Access Interference (MAI) from another user is assumed random. No loss of generality, assuming that desire user is first user ($k = 1$) from medium s with focus on code to- m and subcarrier to- l . Output from coherent matched filter in code to- m and subcarrier to- l from receiver are for user to- l from medium s is

$$z_{1,m,l}^{(s)} = \int_0^{T_s} r(t) \cdot c_1(t) \cos(\omega_l t + \alpha_{k,m}^{(s)}) \quad (11)$$

$\alpha_{k,m}^{(s)}$ is shifting phase in receiver. Output from the previous matched filter can expressed as :

$$Z_{1,m,l}^{(s)} = D_{1,m,l}^{(s)} + N_{1,l}^{(s)} + I_{tot}^{(s)} \quad (12)$$

$$Z_{1,m,l}^{(s)} = D_{1,m,l}^{(s)} + N_{1,l}^{(s)} + I_1^{(s)} + I_2^{(s)} + I_3^{(s)} + I_4^{(s)} + I_5^{(s)} + I_6^{(s)} + I_7^{(s)} + I_8^{(s)} + I_9^{(s)} \quad (13)$$

$N_{1,l}^{(s)}$ is AWGN with *zero mean*, $I_{tot}^{(s)}$ is total interference that caused by code and subcarrier in medium s and medium i , $D_{1,m,l}^{(s)}$ is desired signal for user to- l from medium s in code to- m and subcarrier to- l .

When assumed that the desire signal is the signal from user to- l comes from medium s in code to- m and subcarrier to- l and $\omega_l \gg T_s^{-1}$ hence :

$$D_{1,m,l}^{(s)} = \sqrt{\frac{P_s}{2}} T_s \quad (14)$$

Signal noise $n(t)$ assumed have same spectrum for all the frequency allocated is $N_o/2$ (*two-sided spectral density*) and *zero mean*. Variance noise is given [7].

$$\sigma_n^2 = \frac{N_o}{4} T_s \quad (15)$$

IV. INTERFERENCE VARIANCE

4.1. Interference Variance

4.1.1. Interference from user and from the same medium

- (a) Interference from code and subcarrier from the same user in medium s .

This interference its caused by using of another code and another subcarrier from the same user in the medium s . In the system model, assumed that inter code and inter subcarrier in the same user have orthogonality so that interference will not occur [4]. This case will occur if there is no multipath fading. Assumed the sincronization is perfect and there is no delay path, so the interference that caused by self interference is zero. $I_1^{(s)} = 0$.

- (b) Interference from the same code and the same subcarrier that is used by another user.

This interference is categorize as interference in single-code single-carrier CDMA. If assumed time delay $\tau_k^{(s)}$ distributed uniformly with one bit duration T , ($0 \leq \tau_k^{(s)} \leq T_s$).

$$I_2^{(s)} = \sqrt{2P_s} \sum_{k=2}^{K_s} \int_0^{T_s} b_{k,m,l}^{(s)}(t - \tau_k^{(s)}) c_{k,m}^{(s)}(t - \tau_k^{(s)}) \times \cos(\omega_l t + \phi_{1,l}^{(s)}) c_{1,m}(t) \cos(\omega_l t + \alpha_{1,l}^{(s)}) dt \quad (16)$$

This kind of variance interference is [10]:

$$Var[I_2^{(s)}] = \sum_{k=2}^{K_s} \frac{P_s T_c^2 G_s}{6} \quad (17)$$

- (c) Interference from same code and another subcarrier that is used by another user.

This interference is inter-carrier interference.

$$I_3^{(s)} = \sqrt{2P_s} \sum_{k=2}^{K_s} \sum_{q=1, q \neq l}^L \int_0^{T_s} b_{k,m,l}^{(s)}(t - \tau_k^{(s)}) \times c_{k,m}^{(s)}(t - \tau_k^{(s)}) c_{1,m}(t) \cos(\omega_l t + \phi_{k,l}^{(s)}) \times \cos(\omega_q t + \alpha_{1,q}^{(s)}) dt \quad (18)$$

This kind of variance is [10]:

$$Var[I_3^{(s)}] = \sum_{k=2}^{K_s} \sum_{q=1, q \neq l}^L \frac{6P_s T_c^2 G_s}{4\pi^2 (q-l)^2} \quad (19)$$

- (d) Interference from another code and same subcarrier that is used by another user.

The interference caused by another code from the same subcarrier that used by another user.

$$I_4^{(s)} = \sqrt{2P_s} \sum_{k=2}^{K_s} \sum_{m'=1, m' \neq m}^{M_s} \int_0^{T_s} b_{k,m,l}^{(s)}(t - \tau_k^{(s)}) \times c_{k,m}^{(s)}(t - \tau_k^{(s)}) c_{1,m}(t) \cos(\omega_l t + \phi_{k,l}^{(s)}) \times \cos(\omega_l t + \alpha_{1,l}^{(s)}) dt \quad (20)$$

Variance from this interference is

$$Var[I_4^{(s)}] = \sum_{k=2}^{K_s} \frac{P_s T_c^2}{12G_s} (M_s - 1) \cdot (1 - \frac{\pi^2}{6}) \quad (21)$$

- (e) Interference from another code and another subcarrier that is used by another user.

The interference caused by another code and another subcarrier that used by another user.

$$I_5^{(s)} = \sqrt{\frac{P_s}{2}} \sum_{k=2}^{K_s} \sum_{m'=1, m' \neq m}^{M_s} \sum_{q=1, q \neq l}^L \int_0^{T_s} b_{k,m,l}^{(s)}(t - \tau_k^{(s)}) \times c_{k,m}^{(s)}(t - \tau_k^{(s)}) c_{1,m}(t) \times \cos\left[(\omega_q - \omega_l)t + \phi_{k,q}^{(s)} - \alpha_{1,q}^{(s)}\right] dt \quad (22)$$

The variance from this interference is

$$Var[I_5^{(s)}] = \sum_{k=2}^{K_s} \sum_{q=1, q \neq l}^L \frac{6P_s T_c^2 (M_s - 1) G_s}{4\pi^2 (q-l)^2} \quad (23)$$

4.1.2. Interference from a user in a different medium

- (a) Interference from a different code and different subcarrier that is used by another user.

If assumed that user to- k from medium s that is as a reference user and integrator medium is medium i ($i = 1, 2, \dots, S$), where $i \neq s$ and assumed also that time delay from integrator user $\tau_k^{(i)}$ distributed uniformly with 1 bit period from integrator user is T_i , where $0 \leq \tau_k^{(i)} \leq T_i$.

$$I_6^{(s)} = \sqrt{\frac{P_i}{2}} \sum_{i=1, i \neq s}^S \sum_{k=1}^{K_i} \int_0^{T_s} b_{k,m,l}^{(i)}(t - \tau_k^{(i)}) \times c_{k,m}^{(i)}(t - \tau_k^{(i)}) c_{1,m}(t) \text{Cos } \phi_{k,l} dt \quad (24)$$

Where $\phi_{k,l} = \theta_{k,l} - \omega_l \tau_k$, P_i is received power from user in medium to-1. G_i is processing gain from medium i as an integrator. T_i is bit duration from user in the medium i . This kind of interference is [10] :

$$\text{Var}[I_6^{(s)}] = \sum_{i=1, i \neq s}^S \sum_{k=1}^{K_i} \frac{P_i T_c^3 G_s G_i}{6T_i} \quad (25)$$

(b) Interference from the same code and another subcarrier.

The interference caused by another subcarrier from user in medium i .

$$I_7^{(s)} = \sum_{i=1, i \neq s}^S \sum_{k=1}^{K_i} \sum_{q=1, q \neq l}^L \sqrt{\frac{P_i}{2}} \int_0^{T_s} b_{k,m,l}^{(i)}(t - \tau_k^{(i)}) \times c_{k,m}^{(i)}(t - \tau_k^{(i)}) c_{1,m}(t) \times \text{Cos} \left[(\omega_q - \omega_l)t + \phi_{k,q}^{(i)} - \alpha_{k,l}^{(i)} \right] \quad (26)$$

This kind of variance is [10] :

$$\text{Var}[I_7^{(s)}] = \sum_{i=1, i \neq s}^S \sum_{k=1}^{K_i} \sum_{q=1, q \neq l}^L \frac{P_i T_c^3 G_s G_i}{2T_i \pi^2 (q-l)^2} \quad (27)$$

(c) Interference from another code and the same subcarrier.

The interference caused by another code in the same subcarrier from the user in medium i .

$$I_8^{(s)} = \sum_{i=1, i \neq s}^S \sum_{k=1}^{K_i} \sum_{m'=1, m' \neq m}^{M_i} \sqrt{\frac{P_i}{2}} \int_0^{T_s} b_{k,m',l}^{(i)}(t - \tau_k^{(i)}) \times c_{k,m}^{(i)}(t - \tau_k^{(i)}) c_{1,m}(t) \text{Cos}^2(\omega t) dt \quad (28)$$

Using the process like the interference that is caused by another code and the same subcarrier from another user in the same medium, so that the variance from this interference is

$$\text{Var}[I_8^{(s)}] = \sum_{i=1, i \neq s}^S \sum_{k=1}^{K_i} \sum_{m'=1, m' \neq m}^{M_i} \frac{P_i T_i^2}{12G_i^3} M_i \left(1 - \frac{\pi^2}{6} \right) \quad (29)$$

Substitute the formula of processing gain from another medium G_i to equation (29), hence :

$$\text{Var}[I_8^{(s)}] = \sum_{i=1, i \neq s}^S \sum_{k=1}^{K_i} \sum_{m'=1, m' \neq m}^{M_i} \frac{P_i T_c^3}{12T_i} M_i \left(1 - \frac{\pi^2}{6} \right) \quad (30)$$

(d) Interference from another code and another subcarrier.

The interference caused by another code and another subcarrier from user and from medium i .

$$I_9^{(s)} = \sum_{i=1, i \neq s}^S \sum_{k=1}^{K_i} \sum_{m'=1, m' \neq m}^{M_i} \sum_{q=1, q \neq l}^L \sqrt{\frac{P_i}{2}} \times \int_0^{T_s} b_{k,m',q}^{(i)}(t - \tau_k^{(i)}) c_{k,m'}^{(i)}(t - \tau_k^{(i)}) c_{1,m}(t) \times \text{Cos} \left[(\omega_q - \omega_l)t + \phi_{k,q}^{(i)} - \alpha_{k,l}^{(i)} \right] dt \quad (31)$$

The variance of this kind of interference is

$$\text{Var}[I_9^{(s)}] = \sum_{i=1, i \neq s}^S \sum_{k=1}^{K_i} \sum_{q=1, q \neq l}^L \frac{P_i T_c^3 M_i G_s G_i}{2T_i \pi^2 (q-l)^2} \quad (32)$$

Substitute the desired signal, noise signal, interference from medium s and interference from medium i , so the average Bit Error Rate (BER) equation in medium s is

$$\text{BER}_s = \frac{1}{L} \sum_{l=1}^L \frac{1}{2} \text{erfc}(\sqrt{\text{SINR}}) \quad (33)$$

$$\text{SINR} = \frac{D_1}{\sqrt{\text{Var}[\eta] + \text{Var}[I_{\text{tot}}^{(s)}]}} \quad (34)$$

$$\text{Var}[I_{\text{tot}}^{(s)}] = \text{Var}[I_1^{(s)}] + \text{Var}[I_2^{(s)}] + \text{Var}[I_3^{(s)}] + \text{Var}[I_4^{(s)}] + \text{Var}[I_5^{(s)}] + \text{Var}[I_6^{(s)}] + \text{Var}[I_7^{(s)}] + \text{Var}[I_8^{(s)}] + \text{Var}[I_9^{(s)}] \quad (35)$$

$$\begin{aligned} \text{SINR}^{-1} &= \frac{N_o}{2E_b} + \sum_{k=2}^{K_s} \frac{T_c^2 G_s}{3T_s^2} + \sum_{k=2}^{K_s} \sum_{q=1, q \neq l}^L \frac{3T_c^2 G_s}{\pi^2 T_s^2 (q-l)^2} \\ &+ \sum_{k=2}^{K_s} \frac{T_c^2 (M_s - 1)}{2T_s^2 G_s} \left(1 - \frac{\pi^2}{6} \right) \\ &+ \sum_{k=2}^{K_s} \sum_{q=1, q \neq l}^L \frac{T_c^2 (M_s - 1) G_s}{\pi^2 T_s^2 (q-l)^2} \\ &+ \sum_{i=1, i \neq s}^S \sum_{k=1}^{K_i} \frac{P_i T_c^3 G_s G_i}{3T_i P_s T_s^2} \\ &+ \sum_{i=1, i \neq s}^S \sum_{k=1}^{K_i} \sum_{q=1, q \neq l}^L \frac{P_i T_c^3 G_s G_i}{\pi^2 T_i P_s T_s^2 (q-l)^2} \\ &+ \sum_{i=1, i \neq s}^S \sum_{k=1}^{K_i} \sum_{m'=1, m' \neq m}^{M_i} \frac{P_i T_c^3}{6T_i P_s T_s^2} M_i \left(1 - \frac{\pi^2}{6} \right) \\ &+ \sum_{i=1, i \neq s}^S \sum_{k=1}^{K_i} \sum_{q=1, q \neq l}^L \frac{P_i T_c^3 G_s G_i M_i}{\pi^2 T_i P_s T_s^2 (q-l)^2} \end{aligned} \quad (36)$$

where $E_b = P_s T_s$ and signal to noise ratio is $\text{SNR} = \frac{2E_b}{N_o}$.

V. THE PERFORMANCE OF MULTI-CODE MULTI CARRIER CDMA S-ALOHA

According to its name, Slotted Aloha changes the protocol from continuous time to slotted time. We will observe the time as sequence slot and duration T , where one frame can be sent to each of the slots. In the transmission we assume that the synchronization has occurred, so that all the transmissions can start in the first slot. When a frame is to be transmitted in a time slot, that frame is queued in first time slot. Therefore, one frame competes with another frame that has the same time slot. This reduces the time of contention from two time frames to one time frame. This makes the maximum throughput from Slotted-Aloha two times larger than the maximum throughput of P-Aloha. Traffic load (G) will change according to the time. Note that if the number of packets that are backlogged increases, G will also increase. In this discussion we are assuming that the number of users is unlimited, while the length of the packet being constant. Furthermore we also assume that when a packet arrives, that packet will be transmitted in another slot after. If a collision occurs so a node is backlogged, the backlogged node will transmit the packet in every slot with probability q until success. The number of simultaneous transmissions from the system in a slot duration has been given by the steady state probability from the Poisson process, in this case it follows that

$$P(K, G) = \frac{\left(\frac{G}{M_s \cdot L}\right)^K}{K!} \exp\left(-\frac{G}{M_s \cdot L}\right) \quad (37)$$

$P(K, G_{S-Aloha})$ as a probability in K user that raise $M_s \cdot L \cdot K$ subpacket in one slot duration. $G_{S-Aloha}$ is load traffic, the average of subpacket that sent in one slot duration. The Poisson Model assumes that the number of users are unlimited because generally gives an approximation near to a real condition in a network with many stations.

Systematically throughput value can be written in

$$S = \sum_{k=1}^{\infty} M_s \cdot L \cdot K \cdot P(K, G) \cdot P_a \quad (38)$$

where M_s is the number of code in medium s , L is the number of subcarrier that is used and K is the number of users. P_a is the probability success in transmission of subpacket in the S-Aloha system. It can be written in the form

$$P_a = \left(1 - (BER_s)_{mc-mc}\right)^{L_b} \quad (39)$$

with L_b being the length of a transmitted bit.

VI. RESULT AND ANALYSIS

Based on Figure 1 and 2, we can observe that the performance of throughput in MC-MC-CDMA S-ALOHA with single medium is better than dual medium. This is because in the dual medium system, the interference is caused not only by the code and subcarrier from the same medium but

also because of the code and subcarrier from a different medium.

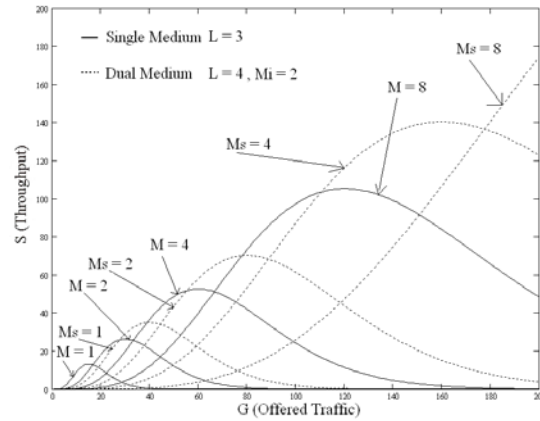


Figure 1. Throughput analysis MC-MC-CDMA S-ALOHA in single medium and dual medium system with $G_s^1 = 32$, $G_i^1 = 64$, $K_s = 200$, $K_i = 50$, $L = 2$, $M_i = 2$, dan M_s in variation

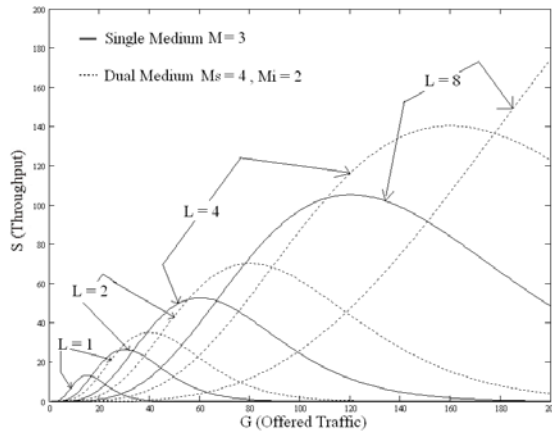


Figure 2. Throughput analysis MC-MC-CDMA S-ALOHA system in single medium and dual medium with $G_s^1 = 32$, $G_i^1 = 64$, $K_s = 200$, $K_i = 50$, $M_s = 2$, $M_i = 2$, and L in variation

VII. CONCLUSIONS

1. Throughput system of multi-code multicarrier CDMA S-ALOHA in dual medium in the AWGN channel has been analyzed
2. Throughput system of multi-code multicarrier CDMA S-ALOHA is better than multi-code CDMA or multicarrier CDMA S-ALOHA system.
3. Throughput system of multi-code multicarrier CDMA S-ALOHA in single-medium is better than dual-medium.
4. Throughput system of multi-code multicarrier CDMA S-ALOHA increases according to the increase in the number of code in medium s (M_s), medium i (M_i) and the number of subcarrier (L).

REFERENCES

- [1] Fu, Hongyi, Mark, Jon W., "Uplink Performance of Asynchronous Multicode Multicarrier CDMA Systems," *IEEE Int. Symposium on Personal Indoor and Mobile Radio Communication Proceedings*, No.14, 2003.
- [2] Lin I, C., Pollini, Gregory P., Ozarow, Larry, dan Gitlin, Richard D., "Performance of Multicode CDMA Wireless Personal Communications Networks," *IEEE Int. Conference on Universal Personal Communication*, vol. 2, hal. 907-911, July, 1995.
- [3] Kim, T., Kim, J., Andrews, Jeffrey G., dan Rappaport, Theodore S., "Multicode Multicarrier CDMA: Performance Analysis," *IEEE Comm. Magazine*, June, 2004.
- [4] Sourour, Essam A., Nakagawa M., "Performance of Orthogonal Multicarrier CDMA in a Multipath Fading Channel," *IEEE Transactions on Communications*, Vol. 44, No. 3, March, 1996.
- [5] Yee, N., Linnartz, J. P., dan Fettweis, G., "Multicarrier CDMA in Indoor Wireless Radio Networks," *Proc. IEEE PIMRC'93*, pp. 468-172, September, 1993.
- [6] Lin I, C., Gitlin, R. D., "Multicode CDMA Wireless Personal Communication Networks," *Proc. ICC '95*, Seattle, W.A., hal. 1060-1064, June, 1995.
- [7] Rappaport, Theodore S., *Wireless Communication: Principles and Practice*, Prentice Hall Inc., NewJersey, 1996.
- [8] Fitzek, Frank H. P., "Quality of Service In Wireless Multicode CDMA System," Technical University Berlin, Telecommunication Networks Group TKN, 05/2002. Berlin, 2002.
- [9] Prasad, R., *CDMA for Wireless Personal Communications*, Artech House Boston-London, 1996.
- [10] Sandouk, A., Harada, M., Okada, H., Yamazato, T., Katayama M., Ogawa, A., "BER Analysis for Multi-Carrier DS CDMA with Multi-Rate Traffic," *IEICE Trans. Fundamentals*, vol. E84-A, No. July, 2001.
- [11] Pursley, M. B., "Performance Evaluation for Phase-Coded Spread Spectrum Multiple Access Communication-Part I: System Analysis," *IEEE Trans. Commun.*, vol. 25, No. 8, hal. 795-799, August, 1977.
- [12] Hu, T. H. dan Liu, M. K., "A New Power Control Function For Multirate DS-CDMA Systems," *IEEE Trans. Comm.*, vol. 47, No. 6, hal. 896-904, June, 1999.
- [13] Hu, Teck H. dan Liu, Max M. K., "DS-CDMA System with Variable-Rate Traffic" *IEEE Communication Letters*, vol. 2, No. 3, hal. 64-66, Maret, 1998.

Dr. Hoga Saragih, ST, MT. was born in Bandung, Indonesia on the 15th of August 1976. He received his Bachelor of Engineering degree in electrical engineering from Christian Krida Wacana University in 1998. He completed his Master of Electrical Telecommunication Engineering from the Department of Electrical a Engineering, University of Indonesia, in 2001. He completed his PhD degree in Electrical Telecommunication Engineering from the Department of Electrical a Engineering, University of Indonesia in 2008. His research interest is in the area of mobile communication, with special emphasis on ALOHA, CDMA. He can be contacted at the following address: Faculty of Computer Studies, Graduate Program in Information Technology (S-2), Bina Nusantara University, Angrek Campus – New Building, th8 floor, Jl. Kebon Jeruk Raya No. 27, West Jakarta, Indonesia 11480. His email address is: hogasaragih@gmail.com

Intelligent Learning Objects (LOs) Through Web Services Architecture

Ahmad Luthfi¹

Faculty of Computer Science
Bina Darma University
Palembang, Indonesia

Abstract— In recent years, e-learning has started to attract a lot of attention from researchers as well as practitioners. Many of the existing architectures for e-learning systems are based mainly on plain client-server or peer-to-peer architectures, and therefore suffer from drawbacks like poor scalability or the complicated interchange of content. In this paper we present a distributed, service-oriented architecture for e-learning systems based on web services, and describe the extensions to support software agents. Moreover, we show what advantages such an architecture may have to offer and propose the usage of intelligent software agents for the distributed retrieval of educational content. The implementation of these services enables a reuse of functionalities of an e-Learning platform. The present research has identified and created common services, which are essential for the creation and authoring stages of typical e-Learning system architecture by utilized Learning Objects (LOs). These services are Web Services based and will provide a common interface between various components leading to platform independence and interoperability between learning system.

Keywords: e-Learning, Web Services, Learning Objects

1. INTRODUCTION

E-learning platforms and their functionalities today resemble one another to a large extent. Recent standardization efforts in e-learning concentrate on the reuse of learning material, but not on the reuse of application functionalities. Our *LearnServe* system builds on the assumption that a typical learning system is a collection of activities or processes that interact with learners and suitably chosen content, the latter in the form of learning objects. This enables us to subdivide the main functionality of an e-learning system into a number of stand-alone applications, which can then be realized individually or in groups as Web services.

The implementation of these services enables a reuse of functionalities of an e-learning platform. The *LearnServe* system is based on common standards, both in the area of e-learning and in the area of Web services. The realization in a distributed fashion leads to a number of challenges including

the maintenance of content and services. However, on the other hand, it has potentials like direct integration of e-learning services into business applications or the access of learning services by different devices if there is an appropriate client for that device.

There are numerous supplementary factors to realize the target and concept of educational technology. For example, the rapid development in information technology has produced faster and better technologies in both hardware and software. As a result, by utilizing them humans beings can improve their skills and work more efficiently.

The Internet provides a distributed infrastructure for sharing information globally, with one estimation that the on-line population will reach 6,300 million users in 2004 [1]. This vast user market becomes a great motivation for the development of new technologies which enables one to build the next generation of the web based application. In particular, the size of the user base makes it attractive to develop collaborative applications that link the growing number of diverse clients with rich media web content.

Many institutions are currently offering courses for tertiary education. In order to pass a course, participants receive a checklist that describes the content of the course. Based on these descriptions, these learners can freely choose content from various providers. Traditional e-Learning platforms do not provide the flexibility that a learner needs in tertiary education. These platforms are usually centralized and offer courses with well-defined or fixed content instead of flexible checklists. Learners do not have the ability to choose from content offered by different authors and styles within a course. Moreover, the content is usually not selectable and adaptable to the specific needs of a learner [2].

A general consensus seems to exist regarding roles played by people in a learning environment as well as regarding the core functionality of modern e-Learning platforms. The main players in these systems are the learners and the authors; others include trainers and administrators. Authors (which can also be teachers or instructional designers) create content, which is stored under the control of a learning management system (LMS) and typically in a database [3, 4].

Existing content can be updated and also reused in other e-Learning systems. The administrator controls the learning management system (LMS). The LMS interacts with a run-time environment, which is addressed by learners, who in turn may be coached by a trainer. The interesting aspect of this

¹Ahmad Luthfi is with Faculty of Computer Science, Bina Darma University, Jl. Jenderal Ahmad Yani No. 12 Palembang 30264, South Sumatera, Indonesia. Email: luthfie@mail.binadarma.ac.id.

An earlier version of this paper was presented at the ICA2009 International Conference in October 2009 in Bandung, Indonesia.

idea is the fact that these three components of an e-Learning system can be logically and physically distributed. That is, they can be installed on distinct machines and offered by different providers or content suppliers. In order to make such a distribution feasible, standards such as IMS and SCORM ensure plug-and-play compatibility to a large degree [5].

E-Learning systems are often not limited to only addressing the needs of a specific learner. They can be implemented in such a way that a customization of features and of the content appearance is adaptable to the needs of the individual learner. Learners vary significantly in pre-knowledge, abilities, goals for approaching a learning system, pace of learning, way of learning, and the time (and money) they are able to spend on learning. To fulfill the needs of such a flexible system, a learning platform has to meet a number of requirements, including the integration of a variety of materials, the potential deviation from predetermined sequences of actions, personalization and adaptation, and the verifiability of work and accomplishments [6].

We consider the approach to construct (standardized) wrappers around e-Learning content as being more promising. In particular, we follow a service-oriented approach that encapsulates educational content inside a Web Service in order to increase interoperability and re-usability. In addition, we also propose a general service-oriented architecture for e-Learning systems, in which the different components are implemented as Web Services [7, 8, 9]. The expected advantages are that system components and content can be distributed all over the Web and offered by different vendors.

Furthermore, the format in which content is stored will be less important, since the Web Services may provide functionality to extract and present it over the Web. For learners, e-Learning systems can be individually assembled by using the distributed components to provide the functionality they really need. We address the problem of content retrieval in such a distributed environment by using intelligent software agents, which take both the preferences of particular users as well as the data into consideration, which is stored inside services. The main focus of the paper is on a general service-oriented architecture for e-Learning systems based on Web Services.

In this paper, we present a mix between literature review and experimentation about e-Learning system, including Web Service Architecture, Learning Object Materials, and the LCMS concept. Moreover, we show the advantages that such a web service architecture may offer and propose the usage of e-Learning System for the distributed retrieval of educational content.

2. E-LEARNING STANDARDIZED

This section briefly introduces some fundamentals relevant to our work, which consists of e-Learning and the Web Services approach.

2.1 E-Learning System

E-Learning has attracted a lot of attention in recent years from researchers as well as practitioners.

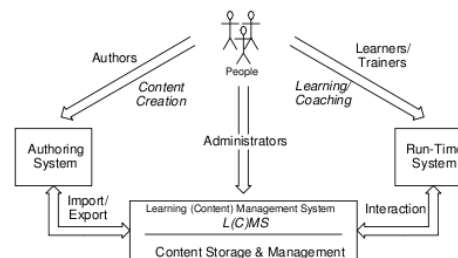


Figure 1. General View of e-Learning System

As depicted in Figure 1, a general agreement exists regarding roles played by people in a learning environment, as well as the functionality of e-Learning systems required in general [9]. In a typical learning environment, there are several groups of people involved: authors and learners, which are the main players, and administrators and trainers. Authors can be teachers or instructional designers who create e-Learning content by using an authoring system.

The core of an e-Learning system, which is under the control of an administrator, typically consists of a learning management system (LMS) or learning content management system (LCMS). An LMS provides functionality like managing learners and their profiles, tracking their progress, easing collaboration, or scheduling events. An LCMS is aimed at managing learning content which is typically stored in a database.

Content consumed by learners and created by authors are commonly handled, stored, and exchanged in units of learning objects (LOs). Basically, LOs are units of study, exercise, or practice that can be consumed in a single session, and they represent reusable granules that can be created independent of the type of delivery medium. The LOs can be accessed dynamically (e.g. over the Web). Ideally, LOs can be reused by different LMS and plugged together to build classes that are intended to serve a particular purpose or goal [10]. Accordingly, LOs need to be context-free, which means that they have to carry useful description information on the type and context in which they may be used. For example, a LO dealing with aching the basics of the SQL language can be used in classes on software engineering, database administration, and data modeling.

The concept of LOs represents one possible solution to the interoperability problem, since LOs are intended for use in many different e-Learning systems. In our view, Web Services represent a suitable technology for the implementation of LOs, since they address a similar problem domain and build on widely spread standards. A collection of Web Services can be employed to handle content and course offerings as well as

other LCMS functionality. We briefly introduce the Web Service paradigm next.

2.2 Web Services

Web Service is a technology that has been developed to provide various types of services over a web connection. The main advantage of using Web Services technology is cross-platform communications. At the start of 2005 there were two major competing technologies in Web Services, namely from Microsoft and Sun Microsystems. As far as implementation is concerned both use common standards and protocols, such as *Simple Object Access Protocol (SOAP)*, *Extensible Markup Language (XML)*, *Web Service Description Language (WSDL)* and *Universal Discovery Description & Integration (UDDI)*. SOAP is an XML-based message exchange protocol that is used to communicate between Web Services and their clients [12]. With the help of this lightweight protocol we can easily exchange structured information in a decentralized distributed environment.

WSDL provides description of a Web Service. Each Web Service has a WSDL file which is basically an XML file that describes a set of SOAP messages the Web Service uses and how the messages are exchanged between Web Services and clients [13]. UDDI is often called the Yellow Pages of Web Services [13]. A UDDI is a directory of Web Services having XML files describing a business and the services it offers. We will use UDDI in our architecture.

In essence, Web Services are independent software components that use the Internet as a communication and composition infrastructure. They abstract from the view of specific computers and provide a service-oriented view by using a standardized stack of protocols. In a typical invocation of a Web Service, a client may use a UDDI registry and the UDDI protocol to find a server that hosts a service. It then requests from the server a WSDL document written in the Web Services Description Language, which describes the operations supported by the service. For the invocation, the Simple Object Access Protocol (SOAP) protocol can be used, which builds upon HTTP to transport the data. More complex Web Services can be composed out of existing services using, for example, BPEL4WS. For more details on Web Services we refer the reader to [11].

2.3 Web Services Architecture

In a Web Service-based computing model, both clients and Web Service providers are unaware of implementation details. If the client wants to consume a Web Service, the client will need to go through four stages. These four stages are directory, discovery, description and data which is also called the wire format [13]. Figure 1 presents a Web Service infrastructure. At the first stage (directory), a client searches for a Web Service. Directories services such as UDDI provide a central place for storing published information about Web Services. The client searches a directory and finds a URL.

In the second stage a client sends a request for service description documents. The server returns the discovery document that enables the client to know about the presence

of a Web Service and its location. In the third stage the client sends his request for a particular Web Service. The service description is sent by the server in XML which specifies the format of the messages that the Web Service can understand [14].

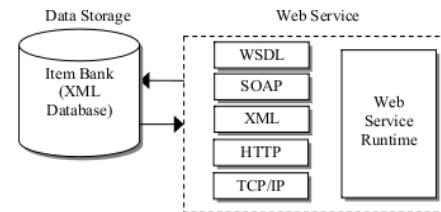


Figure 2. System Architecture

Figure 2 shows the overall architecture by applying a SOA concept. The architecture is separated into the two parts: data storage and Web Service. In data storage, the XML database stores items. An item bank data structure is described in an XML document. The item structure is a subject to a XML schema developed according some defined standards. This database structure is designed by using the basic data structure of the general testing parameters, such as question, multiple choice, and answer.

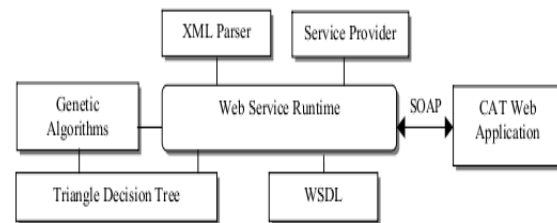


Figure 3. Web Service Architecture

In Web Service design, a set of standards for describing, publishing, discovering, and binding application interfaces is defined using WSDL, SOAP and UDDI. WSDL is a format for describing a Web Service interface [15]. It describes services and a way they should be bound to specific network addresses. The descriptions of services and messages are generally expressed in XML. SOAP provides the envelope for sending messages via the Internet (Figure 2).

UDDI defines a set of services supporting the description and discovery of service providers. The design of Web Service consists of four main modules – GAs, TDT, SOAP, and WSDL – as shown in Figure 3. The Genetic Algorithms (GA) are the item classification method to generate an optimal decision tree.

As shown in Figure 4, *LearnServe* is divided into two parts: a client software and Web services provided by several suppliers. The *LearnServe* client is the access point for users who can use the learning services. These services are implemented on distributed servers and in particular include authoring, content, exercise, tracking, a discovery services as well as communication services such as email and message

boards. The exercise services are provided by our *xLx system* [21], that was enhanced to offer its functionality as a Web service and can thus already be used in external systems.

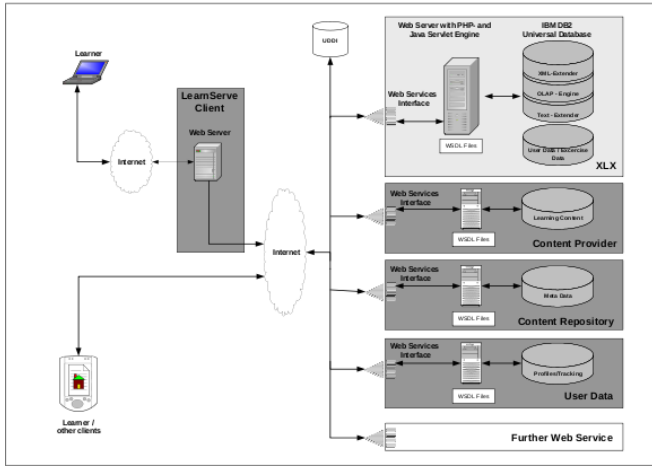


Figure 4. High Level Web Services Architecture

3. RESULTS

3.1 Web-Services-Based LCMS

In this section we present a service-oriented architecture of an LCMS based on Web Services, which is extended to support software agents. We assume that all the LCMS functionality including, the learning contents, are implemented as Web Services.

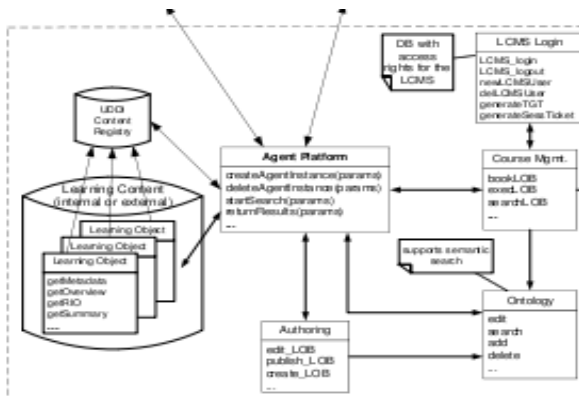


Figure 5. Learning Content Management System

In this Figure 5, Web Services are depicted as rectangles containing a name as well as the most important operations. Furthermore, the architecture is designed in such a way that a learner only needs an Internet browser to use the LCMS. We explain the architecture shown as well as most of the operations listed in this figure in more detail in the following subsections.

3.2 LCMS Architecture

The architecture of our LCMS is aimed at coordinating all learning-related activities and the management of learning materials. The PC computer of a learner interacts directly with the LCMS during a learning session [9]. All Web Services of the LCMS should also be accessible via Web pages, so that the learner only needs a Web browser to utilize the LCMS.

In a first step the learner has to authenticate in the LCMS, which is done by a LCMS login service. This service draws on a database with access rights and uses an authentication mechanism. When the learner is logged in and authenticated, he or she can access a Web page for course management, the functionality of which is implemented as a course management service. The learner can look for suitable courses with a *searchLOB* operation, which searches for learning objects with the help of the agent platform, also implemented as a Web Service. The *bookLOB* operation is called to enroll for a course that was found by an agent. A class can be attended by calling the *execLOB* operation on the remote LO.

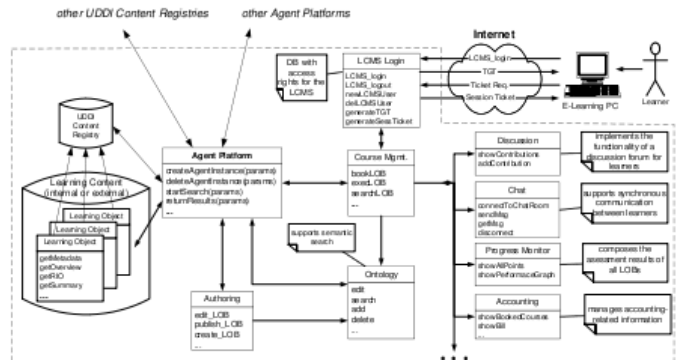


Figure 6. Components of a distributed, Web-Services-Based LCMS

The LCMS may also comprise of other services. In discussion boards or chat rooms learners can interact with instructors or other learners and ask questions. A progress monitor composes the assessment results from all lessons into a general overview; this can also be used to create certificates. An accounting service manages all processes which are related to financial aspects. It shows, for example, all booked courses or the bill that has to be paid by an individual. Finally, it should be mentioned that the functionality of the LCMS can be extended by other Web Services, which can either be provided internally (i.e. in a local network) or externally from other suppliers over the Web.

3.3 Learning Objects (LOs) and Metadata

Learning objects (i.e. educational content) is provided in form of Web Services. In general, LOs may have any desired structure. From a conceptual point of view, however, LOs typically contain parts like Metadata, Overview, Summary and one or more Reusable Information Objects (RIOs), which in turn contains a content part, a practice items part, and an assessment items part for the generation of online tests [3]. In addition to traditional LOs, Web-service-LOs come with operations to extract, manipulate, and present contents.

Therefore, the format in which content is stored inside a Web Service is less important. Operations might even be invoked to randomly generate online-tests from the assessment items.

The agent platform is an environment in which software agents can be executed to retrieve LOs, and which is wrapped by a Web Service. Agents are intended to assist learners with a focused search for LOs, according to the specifications they make. The search parameters of an agent, the start of a search, or the access to the list of retrieved LOs, for example, can be controlled by invoking appropriate Web Service operations which extract metadata from LOs.

Learning objects can be stored in a relational or an object-relational database and are typically a collection of attributes, some of which are mandatory, and some of which are optional. In a similar way, other information relevant to a learning system (e.g. learner personal data, learner profiles, course maps, LO sequencing or presentation information, general user data, etc.) can be mapped to common database structures. This makes interoperability feasible; moreover, it allows for a process support inside an e-Learning system that can interact with the underlying database appropriately [10, 17].

Metadata in reality is data describing data and it can be used to describe any digital resource. There are various metadata elements which describe different aspects of digital resources. For example the IEEE LOM specification [17] has metadata elements which enable the description of digital resources. Such descriptions include amongst other things the purpose of the resource, technical information about the resource, and the ownership of the resource. The ownership of the resource is described by digital rights metadata tags [18].

4. CONCLUSION AND DISCUSSION

Many custom e-Learning platforms can only present their material inside the platform, while on the other hand Internet-based Web Services are becoming ubiquitous, both at a professional and at a personal level. A service-oriented e-Learning system results from a perception of the various tasks and activities that are contained in such a system as processes or as work-flows; using appropriate encodings of objects and tasks in UDDI and WSDL forms and documents enable broad exchanges, flexible compositions, and highly customized adaptations possible.

We also identified the essential services in the functioning of a typical e-Learning based. These services (with real time Web Services technology) would provide a common interface between various components leading to platform independence and interoperability between learning systems.

REFERENCES

- [1] Global Internet Statistic, <http://www.greach.com/globalstats/index.php3>
- [2] Westerkamp, P., *e-Learning as a Web Service*. University of Munster, 2005
- [3] Husemann, B., J. Lechtenborger, G. Vossen, P. Westerkamp. "XLX - A Platform for Graduate-Level Exercises", in *Proc. Int. Conf. on Computers in Education*, Auckland, New Zealand, December 2002, pp. 1262-1266.
- [4] IEEE Standards Department (2002). *Draft Standard for Learning Object Metadata*. IEEE Publication P1484.12.1/D6.4, March 2002.
- [5] Advanced Distributed Learning Initiative (2001). *Advanced Distributed Learning Sharable Content Object Reference Model*, the SCORM Overview, Version 1.2
- [6] Casati, F., U. Dayal, eds. (2002). Special Issue on Web Services. *IEEE Bulletin of the Technical Committee on Data Engineering*, 25 (4), December 2002.
- [7] Pankratius, V., Sandel, O., and Stucky, W. "Retrieving Content with Agents in Web Service E-Learning Systems", *Proc. of the Symposium on Professional Practice in AI*, IFIP WG12.5, First IFIP Conference on Artificial Intelligence Applications and Innovations (AIAI), Toulouse, France, August 2004.
- [8] Harrer A., "Software Engineering Methods for the Reuse of Existing Components in Educational Systems", *Proc. International Symposium on Artificial Intelligence and Applications*, 2002, 430-435.
- [9] Pankratius, V. *E-Learning Grids: Exploitation of Grid Computing in Electronic Learning*, Masters Thesis, Dept. of Information Systems, University of Muenster, Germany, 2003.
- [10] Vossen, G., P. Jaeschke (2002). Towards a Uniform and Flexible Data Model for Learning Objects. In *Proc. 30th Annual Conf. of the Int. Bus. School Computing Assoc. (IBSCA)*, Savannah, Georgia, July 2002, pp. 99-129.
- [11] Booth, D., Haas, H., et. al (eds.), "Web Services Architecture", W3C Working Draft 11 February 2004. <http://www.w3.org/TR/2004/NOTE-ws-arch-20040211/>
- [12] Aaron S. (2003), *Understanding SOAP*, MSDN Library Articles, Microsoft Corporation. <http://msdn.microsoft.com/webservices/default.asp>
- [13] Roger W. (2001), *XML Web Services Basics*, MSDN Library Articles, Microsoft Corporation <http://msdn.microsoft.com/webservices/understanding/webservicebasics/default.asp>
- [14] Hussain, N. and Khan, M. K., *Enhancing E-Learning through Web Service and Intelligent Agents*, 2005.
- [15] Phankokkrud, K. Woraratpanya, "Web Service Architecture for Computer-Adaptive Testing on e-Learning", *Proceedings of World Academy of Science, Engineering and Technology*, Volume 36, December 2008, ISSN 2070-3740.
- [16] Learning Management Systems and Learning Content Management Systems De-mystified, <http://www.brandonhall.com/public/resources/lms lcms/>
- [17] LOM - Draft Standard for Learning Object Metadata, IEEE 1484.12.1-2002, 15 July 2002
- [18] Mohan, P. and C. Brooks, "Learning Objects on the Semantic Web", *Proceedings of International Conference on Advanced Learning Technologies*, Athens, Greece, 2003
- [19] Manouselis, N. and D. Sampson, "Agent-based e-Learning Course Discovery and Recommendation: Matching Learner Characteristics with Content Attributes",

International Journal of Computers and Applications (IJCA), Special Issue on Intelligence and Technology in Educational Applications, Volume 25, Issue 1, January 2003

- [20] Mataric, M., "Interaction and Intelligent Behavior", MIT, Cambridge, USA, 1994.
- [21] Wasterkamp, Peter. "e-Learning as a Web Services". University of Munster, Germany. 2007.



Ahmad Luthfi, S.Kom., M.Kom., born in Curup (Bengkulu) March 11th 1976, holding a Master Degree in Computer Science from Gadjahmada University in 2005 and also a Bachelor Degree in Information System from Bina Darma University in 1999. He is currently head of Information Technology Study Program for Bachelor and Master Degree program in Bina Darma University. He is also focus on several Field of research studies such as Semantic Web, Ontology concepts, and

Intelligent Learning Management System, which published in several journal and proseding national and also international level including KNSI, SNEIE, SNATI, ICTS, ICA, and ICTS.

Industrial Control Quality Improvement using Statistical Process Control: Tennessee Eastman Process Simulation Case

Endra Joelianto¹ and Linda Kadarusman²
Bandung Institute of Technology
Bandung, Indonesia

Abstract—Industries need quality control as it can help to decrease operation cost, to improve product quality, etc. Quality control can be established by controlling the quality of raw materials, controlling of process variable by using control systems (such as PI/PID controller), and so on. A well known method that can be used to measure the performance of the controlled variables is the *Statistical Process Control (SPC)*. In this paper, the operation cost, the product quality, process pressure, and production rate from the Tennessee Eastman process simulation were evaluated by using SPC method. The Tennessee Eastman process was simulated by using SIMULINK and MATLAB 7.01 software. Besides evaluation, the control system design from outcome tuning parameters controller PI was studied.

Keywords: *PI/PID Controller, Statistical Process Control, Process Simulation*

1. Introduction

Quality control is important to industries as it can decrease defective products, reduce operations cost, and improve product quality. Quality control can be established by controlling the quality of raw material, controlling the process variable use controller (such as PI controller), and others. Previously quality control was only conducted at final stages of a product. This resulted in various losses, such as loss of consumer trust, many unsold defective products, increase in operation cost, and other negative impacts. A method that can be used to monitor quality controlling is known as Statistical Process Control (SPC) [1-3].

SPC softwares are usually are located in the office level which is used to assess the performance of the process industries. In the past, such approaches were difficult to implement. However, with the technological advances within the industrial automation systems driven by advancement of communication and networking technologies, this task now can be performed easily. The important software in interfacing data from the field level to the office level is the *Open Process*

Control (OPC) software. Today the data from the sensors and actuator in the field level can be easily located within a single database, which allows an easier review of entire operational performance and trends (rather than unit by unit) from a single location. Collected data may also be used to document environmental regulatory compliance. Integration of plant data with business applications will automatically provide informed business decisions. Long-term data storage enabling high volumes of data can be analyzed to ensure best practices to achieve the best quality product and to minimize energy consumption, while incidents can be analyzed and avoided.

At the network level, today process automation intensively uses computer network technologies and intelligent sensors and actuators. Communications in process automation is now dominated by the Ethernet protocol, replacing the old serial communication using RS 232 or RS 485. Many vendors have developed the Ethernet version of their communication protocol in order to gain faster transmission over the old serial transmission. Latency tests of Ethernet has shown faster data transmission rates than RS 485 by using the Modbus protocol [4]. Many advantages and new different ways of performing transparent process automation using the Ethernet have been developed by vendors. This will improve the implementation of plant-wide control using advanced control methods that needs real-time process variables for comprehensive, fast and accurate compensation.

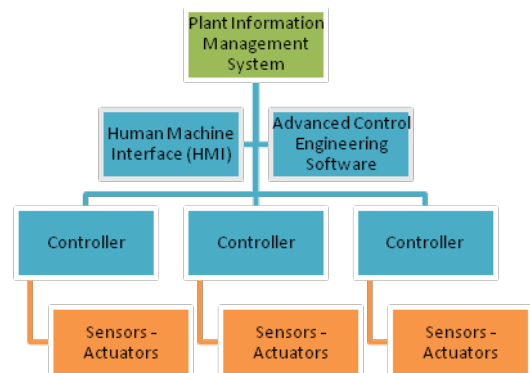


Figure 1: Transparent Process Automation Hierarchy

Figure 1 shows the transparent process automation hierarchy by using Ethernet and OPC technology denoted by the blue line. By using these technologies, engineers can perform not only the calculation for the controllers but can

¹ Endra Joelianto is with the Bandung Institute of Technology (ITB), Jalan Ganesha 10, Bandung 40132, Indonesia. E-mail: ejuel@tf.itb.ac.id.

² Linda Kadarusman is also with the Bandung Institute of Technology (ITB), Jalan Ganesha 10, Bandung 40132, Indonesia.

An earlier version of this paper was presented at the ICA2009 International Conference in October 2009 in Bandung, Indonesia.

also directly manipulate the controller by using many engineering science calculation softwares and optimizations. The SPC software in the plant information management system also gain benefits from this network communication as it can be incorporated to the advanced control engineering software and the human machine interface (HMI), to gather data and to deliver the results to the controllers. Moreover, Ethernet communications is now being developed to replace the conventional analog signal transmission from the controller to sensors and actuators and vice versa, denoted in Figure 1 by the orange lines. By using faster industrial data communication, integrated monitoring and control systems over a wider plant area can be applied to perform better process production beyond the conventional industrial data transmission using analog signal.

Plant-wide control within Tennessee Eastman (TE) is an interesting and challenging problem in industrial process control. The TE problem was first proposed by Downs dan Vogel in 1993 [5]. The problems include multivariable process control, multi objective optimization, adaptive and predictive control, interacting control, nonlinear control, identification and estimation, diagnostic and monitoring, education, and others. Since the TE problem was accepted as a standard experimental apparatus in plant-wide control design, more than 60 papers have been published internationally. The TE process represents a process simulator which mimics the real process. The diagram block of the TE process is shown in Figure 2. The process consists of many units, such as an exothermic reactor, a two-phase reactor, a flash separator and a reboiler stripper. In this TE process, there are 41 measured output variables and 12 manipulated variables. Using the TE process, various research from different perspectives and various control methods – with many different level of difficulties and complexities – can be conducted close to the real process [6,7].

The objectives of this paper are to evaluate operation cost, product quality, process pressure, and production rate from Tennessee Eastman process simulation, and to study control system design from the outcome tuning parameter controller PI by using SPC method. The outlined problems are: the system is linear system so there is no disturbance in simulation process, the simulation process is a simplified process (MATLAB with Fortran to simulink), the quality product is focused on G product composition, the analysis is done off-line, and the process is viewed from overall perspective.

The Tennessee Eastman process is provided by using basic control system as shown in Figure 2. In this paper, the Tennessee Eastman process is viewed from overall perspective (Figure 3) and simulated by using SIMULINK and MATLAB 7.01 based on simulation process developed by Ricker, 2000 [8]. In every stream of the Tennessee Eastman process, overall process uses PI controller where K_c and I denote the gain and the integral parameters respectively [9]. The simulation process is divided into 2 sections, the preliminary and the main sections.

In the introduction section, based on the Tennessee Eastman overall process, the controller parameter value was changed. Controller parameter values are increased by multiplying with 100 and decreased by dividing with 100

from the default controller parameter values. First, the process is simulated with no controller parameter change (called the default condition). Then one of the controller parameter process value is increased from the default parameter value and the simulation is repeated from the start. Next, the other controller parameter process value is decreased from the default parameter value and the simulation is repeated from the start. But the other controller parameter value is still at default value. The simulation result when the parameter values are at the default, increased, and decreased states were collected for the SPC analysis.

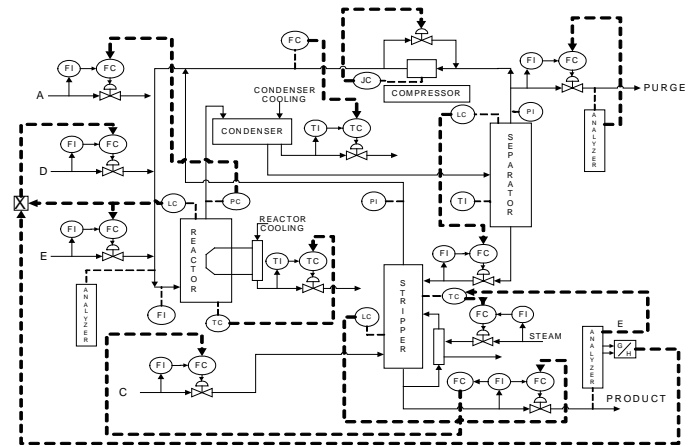


Figure 2: Tennessee Eastman Process Scheme with Basics Controlling (McAvoy, Ye, 1994) [6]

Sample from data of each simulation was taken every 1 hour and UCL and LCL for control chart (\bar{x} and MR chart) was calculated using equations below with n is 3:

For \bar{x} chart :

$$\bar{x} = \frac{\sum_{i=1}^N x_i}{N} \quad (1)$$

$$UCL = \bar{x} + E_2 \overline{MR} \quad (2)$$

$$\text{centre line (CL)} = \bar{x} \quad (3)$$

$$LCL = \bar{x} - E_2 \overline{MR} \quad (4)$$

For MR chart :

$$MR = \text{range from } x_i \text{ until } x_{i+n} \quad (5)$$

$$UCL = D_4 \overline{MR} \quad (6)$$

$$\text{centre line (CL)} = \overline{MR} \quad (7)$$

$$\text{LCL} = D_3 \overline{MR} \quad (8)$$

The constants are given in Table 1 in the following.

Table 1 Constants for x chart and MR chart (Smith, 1998) [2]

n	D_3	D_4	E_2
2	0.000	3.267	2.659
3	0.000	2.574	1.772
4	0.000	2.282	1.457
5	0.000	2.115	1.29

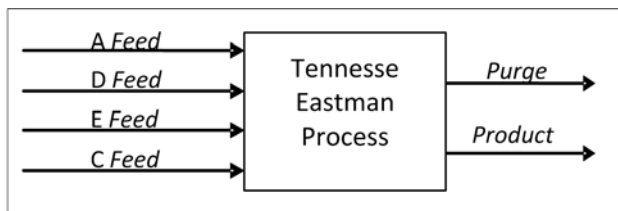


Figure 3: Tennessee Eastman Overall Process Scheme (McAvoy, Ye, 1994) [5]

2. Simulation Procedures

Simulation is carried out by using the TE process simulation software developed in [8]. After simulation, each controller parameter value was studied and the controller parameter values that give the best state and the worst state based on control chart criteria are selected.

Results are then analyzed by comparing operation cost, product quality, process pressure, and production rate control chart between the controller parameter values at default condition and at change value conditions. In the introduction section, the compared control charts are obtained when the controller parameter values are at default, increased, and decreased conditions. Next, the controller parameters that give significant difference in the control chart at 3 conditions for Tennessee Eastman overall process are called influential controller parameters. In the main section, the compared control charts are the control chart where every controller parameter value is at changed condition with control chart at the default condition.

The Tennessee Eastman process is viewed from the overall perspective to decrease controller parameter which is then tested. The tested controller in the introduction section are the controller at A, C, D, and E feed rate, purge rate, production

rate, and %G in product in Figure 3, with the controller parameter K_c and τ_I . The influential controller parameters which resulted from the introduction section are the A feed rate controller K_c and τ_I parameters, C feed rate controller K_c and τ_I parameters, production rate controller K_c parameters, purge rate controller K_c and τ_I parameters, %G in product controller K_c and τ_I parameters.

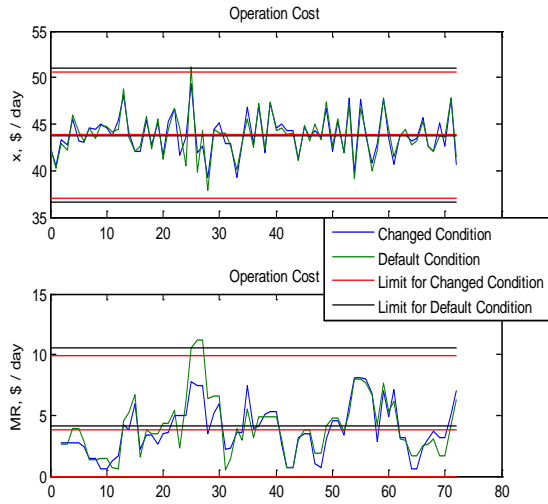
In the main section, the value of each controller parameter that were resulted from the introduction section is then changed. Next, from the main section result, the parameter values of each controller that give the best and the worst condition is selected. The criteria for the value selection of each controller parameter that give best condition are given in the following:

1. It does not pass LCL and UCL, for x and MR chart, and for operation cost, product quality, pressure and production rate.
2. It has lower operation cost average, or higher product quality average, or pressure average that more closer to set point (2800 kPa), or higher production rate average than default condition.

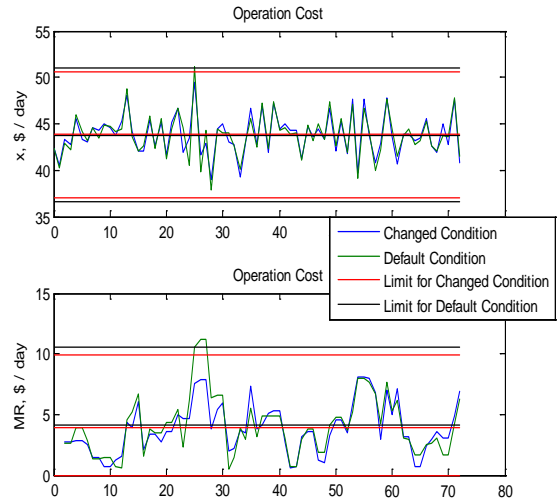
The criteria for the worst condition is opposite to the criteria for the best condition.

3. Analysis and Results

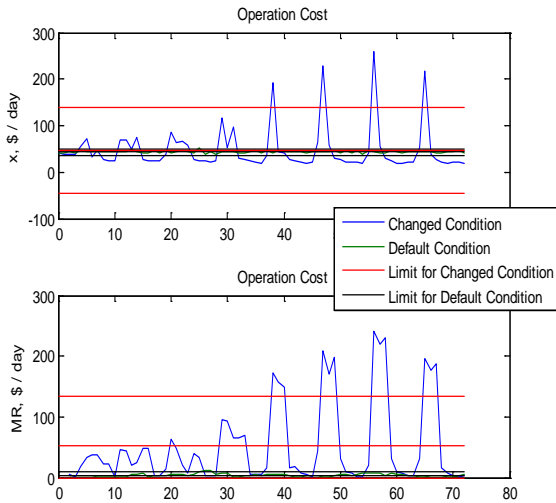
Result analysis was done by comparing the operation cost, product quality, process pressure, and production rate control chart between the controller parameter change value condition with the default condition. In the introduction section, the control chart that was compared are the controller parameter values at default condition, at increased value condition, and decreased value condition. Example of the control chart from the introduction section result is τ_I parameter for %G in product controller shown in Figure 4(a) at the increased controller parameter value condition, and Figure 4(b) for the decreased controller parameter value condition. In the main section, the control chart that was compared are the controller parameter values at the default condition and the changed value condition. The results of the value selection of the controller parameters from the main section are shown in Table 2. Example of the control chart from the main section result is τ_I parameter for %G in product with best condition shown in Figure 5.



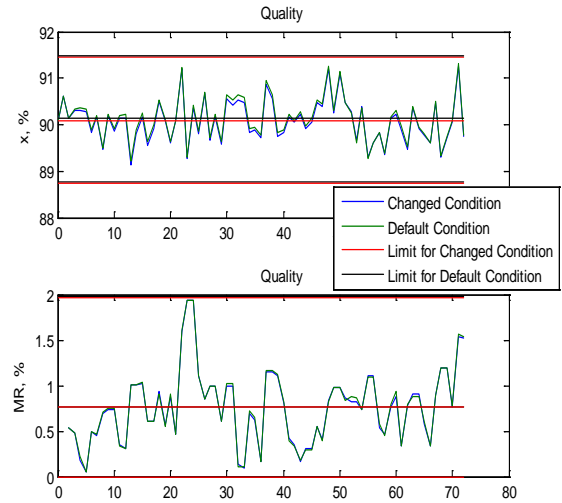
(4a)



(5a)

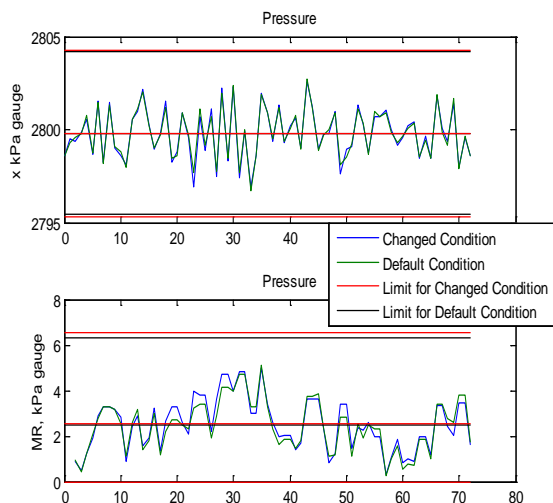


(4b)

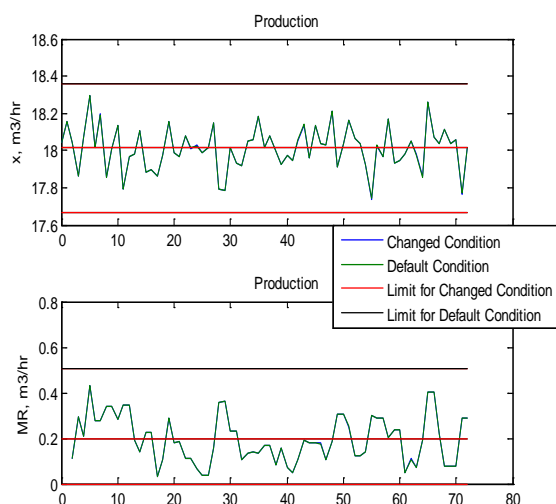


(5b)

Figure 4: Example of Control Chart (x and MR Chart) from the Introduction Section Result When Controller Parameter at (a) decreased value condition, (b) increased value condition



(5c)



(5d)

Figure 5: Example of Control Chart (x and MR Chart) from the Main Section Result for: (a) Operation Cost, (b) Quality, (c) Pressure, (d) Production Rate.

Based on the Tennessee Eastman overall process perspective, it was observed that not all PI controller parameter shows significant effects in operation cost, quality, pressure, and production rate between condition at changed value controller parameter and condition at default value controller parameter. The controller parameters on overall process that had significant influence are A feed rate controller K_c and τ_I parameter, C feed rate controller K_c and τ_I parameter, production rate controller K_c parameter, purge rate controller K_c and τ_I parameter, %G in product controller K_c and τ_I parameter. The operation cost at the default condition (controller parameter have not changed yet) passed UCL for x and ME chart.

Table 2: Each Controller Parameter Value for Default, Best, and Worst Condition from the Main Section Result

Controller	Default Condition		Best Condition		Worst Condition	
	K_c	τ_I	K_c	τ_I	K_c	τ_I
A feed rate	0,01	0,001 / 60	1	0,00001 / 60	0,000333	0,03 / 60
C feed rate	0,003	0,001 / 60	0,0003	0,01 / 60	0,000033	0,09 / 60
Production rate	3,2	—	0,32	—	128	—
Purge rate	0,01	0,001 / 60	0,9	0,000011 / 60	0,000167	0,06 / 60
%G in product	-0,4	100 / 60	-0,04	1000 / 60	-4	11,11 / 60

A feed rate controller (K_c) parameter and %G in product controller (τ_I) parameter show significant tendency when their value was increased such that the control chart would not pass their limit and when their value of parameter was decreased so that the control chart would pass their limit. A feed rate controller τ_I parameter showed tendency when the controller parameter value was increased such that the control chart would pass their limit and when the value was decreased such that the control chart would not pass their limit. C feed rate controller K_c and τ_I parameter, production rate and %G in product controller K_c parameter, purge rate controller K_c and τ_I parameter did not show any tendency in the control chart.

Value changing of each parameter values of the controller could give better chart result (x and MR) than the default value condition. Control chart can be used to provide easier overview of the process and the offset for chemical industry like Tennessee Eastman process. If the range value between UCL and LCL in control chart is smaller, then the system response reaches the set-point with less oscillation. Only the purge rate controller with K_c and τ_I parameter at the best condition that gave lower operation cost average than at the default condition and the other controller parameter at best condition.

4. Conclusions

The Tennessee Eastman process has been investigated from the plant wide control consideration by using statistical process control analysis. By using SPC, the Tennessee Eastman process can be evaluated and studied so the controller parameter values that gave better result than the default condition on operation cost, product quality, process pressure, and production rate can be obtained. In the future, it would be better if the controller parameter values were changed with particular selected parameters that can give better results, particularly on operation cost. Moreover, the investigation needs to include the effect of the set point value used in the process.

Notation

x	sample
\bar{x}	sample (x) average
\overline{MR}	Moving Range average
LCL	Lower Control Limit
MR	Moving Range sample
n	number of sample that use to calculate a MR
N	number of sample
UCL	Upper Control Limit

Endra Joelianto (M'01) received the B.Eng. degree in Engineering Physics from Bandung Institute of Technology, Indonesia in 1990, and Ph.D. degree in Engineering from The Australian National University (ANU), Australia in 2002. He was a Research Assistant with the Instrumentation and Control Laboratory, the Department of Engineering Physics, Bandung Institute of Technology, Indonesia from 1990-1995. Since 1999, he has been with the Department of Engineering Physics, Bandung Institute of Technology, Bandung, Indonesia, where he is currently an Assistant Professor. His research interest includes hybrid control systems, discrete event systems, artificial intelligence, robust control and intelligent automation. He has edited one book on intelligent unmanned systems published by Springer-Verlag, 2009 and published more than 70 research papers. Dr. Joelianto currently is an Editor of the International Journal of Artificial Intelligence (IJAI). He is the Chairman of Society of Automation, Control & Instrumentation, Indonesia. He was the General Chair of the International Conference on Instrumentation, Control and Automation, Bandung 2009.

REFERENCES

- [1] Berger, Roger W. and Thomas Hart (1986), *Statistical Process Control, A Guide for Implementation*, Marcel Dekker, Inc., New York.
- [2] Smith, Gerald M. (1998), "Statistical Process Control And Quality Improvement, 3rd edition", Prentice Hall International, USA
- [3] Montgomery, Douglas C. (2001), *Introduction to Statistical Process Control*, 4th edition", John Wiley & Sons, Inc., USA
- [4] Joelianto, E. and Hosana (2009), "Loop-Back Action Latency Performance of an Industrial Data Communication Protocol on a PLC Ethernet Network", *Internetworking Indonesia Journal*, Vol.1, No.1, pp. 11-18.
- [5] Downs, J. J. and E. F. Vogel (1993), "A Plant-Wide Industrial Control Problem", *Comput. Chem. Engng.*, 17, pp. 245-255.
- [6] McAvoy, T. J. and N. YE (1994), "Base Control for The Tennessee Eastman Problem". *Comput. Chem. Engng.*, 18, pp. 383-413.
- [7] McAvoy, T. J. (2002), "Model Predictive Statistical Process Control of Chemical Plant", In *Proceeding of the American Control Conference*, pp. 3876-3881, Anchorage.
- [8] Ricker, N. Lawrence, (2000), <http://www.eas.asu.edu/~cse1/Software-TennEast.htm>
- [9] Stephanopoulos, George (1984), *Chemical Process Control, An Introduction to Theory and Practice*, Prentice/Hall International, Inc., New Jersey.

FPGA Simulation of AD Converter by using Giga Hertz Speed Data Acquisition for Partial Discharge Detection

Emilliano, Chandan Kumar Chakrabarty, Ahmad Basri,
Agileswari K. Ramasamy, Lee Chia Ping

Department of Electronic and Communication Engineering, College of Engineering (COE)
Universiti Tenaga Nasional
Km.7, Jln.Kajang-Puchong,43009, Selangor Darul Ehsan, Malaysia
emilliano@uniten.edu.my, Chandan@uniten.edu.my

Abstract- Currently, FPGA (Field Programmable Gate Array) technology is being widely used for accelerator control owing to its fast digital processing capability. This paper is purely a model to determine the design circuit to implement Partial Discharge (PD) detection in FPGA technology. The research shall involve ISE Simulator version 9.2i (Xilinx) and Very high integrated circuit Hardware Description Language (VHDL) programming to evaluate the use of Field Programming Gate Array (FPGA) for the detection and counting of partial discharge signals in underground cable. The impulse signals at the input data have very fast rise time in the range of 1 ns to 2 ns.

Keyword- Partial Discharge Detection, FPGA Simulation, FPGA Technology, ADC with Peak Detector Block, Real Time Processing, Underground Cable, Counter with Reset Block, VHDL Programming.

I. INTRODUCTION

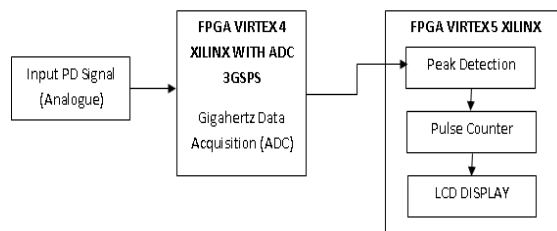


Fig. 1 Block Diagram Partial Discharge Detection using Gigahertz Data Acquisition with FPGA Technology

FPGA compiler use (Test Bench) Xilinx ISE simulator and Xilinx Synthesis Technology (XST) to process synthesis and simulate real time data from output Analogue to Digital Converter (ADC) block to Peak Detection Block, and then process counting PD signal in Impulse Counter with Reset Block (30 bit). The impulse PD signals at the input data have very fast rise time in the range of 1 ns to 2 ns. Fig.1 shows the typical block diagram for detecting and monitoring partial discharge signal.

PD detection system is an automatic system that can detect and display PD signals from underground cable for easy readout. PD detection system can work without oscilloscope, computer or any other associated costly measuring equipment. PD signal is detected by using magnetic probe sensor. This

system can detect the PD signal in underground cable from above the ground without outage.

A Partial Discharge (PD) is a flow of electrons and ions which occurs in a gas over a small volume of the total insulation system. This short duration series of events or impulse emit acoustic, optical, electrical and electromagnetic energy. PDs can be detected by measuring any of this radiation energy.[1]

The work in this paper primarily involved modeling, which comprises a FPGA compiler ISE Xilinx Synthesize Technology (XST) and ISE Xilinx simulator approach whereby the impulse signals will be processed, detected and counted using ADC with peak detector block and counter with reset block. In the next stage, this method will be implemented on a lab simulation scale for testing and validation. With this method of PD detection, real PD signals can be detected although the PD signals from magnetic probe sensor are too weak. The PD signals can also be counted and displayed clearly even if the PD signals have too much distortion.

The functional approach of the ADC with peak detector block and counter with reset block will be dealt in this paper. The physics of PD generation and data acquisition system are very extensive and broad. Thus, they are not dealt in this work.

In short a PD gives rise to voltage and current pulses with time durations in the range of a few nanosecond (ns), travelling at velocity of electromagnetic waves. Due to the high sensitivity of magnetic probes, the shape of the pulse is preserved with very high integrity.

II. DESIGN BLOCK OF THE PD DETECTION

Fig. 2 shows the functional approach of the ADC with peak detector block and impulse counter with reset block in the overall processing layout to count the PD signals. Other blocks such as latch data block, reset automatic block and driver LCD block are not dealt in this work.

A. Block ADC and Peak Detector

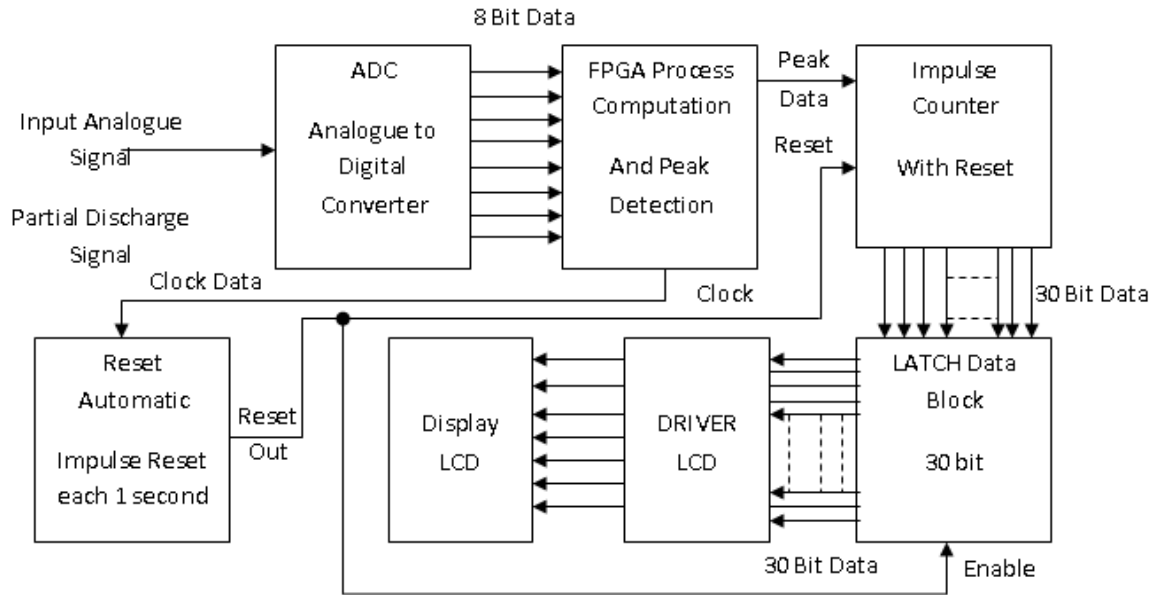


Fig. 2 All Schematic Diagram of Block Diagram Partial Discharge Detection using FPGA

The function of ADC is to convert analogue signals to digital signals by sampling time, and digitize signal. FPGA with ADC is used as the real board integrates these two components. The purpose of the FPGA and the ADC converter is for counting the amount of PD signals from ADC signal in the FPGA and then perform the computation of the real time data using intelligence algorithm in VHDL Programming. Fig. 3 shows the input PD signals.

Analogue Signal of Input Partial Discharge Signal:

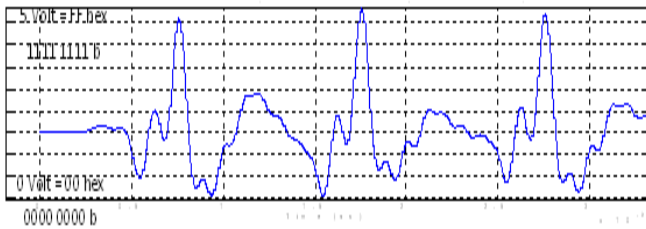


Fig. 3 Input Data Analogue from ADC

A.1. Block Diagram ADC:

Fig. 4 shows the block diagram data ADC.

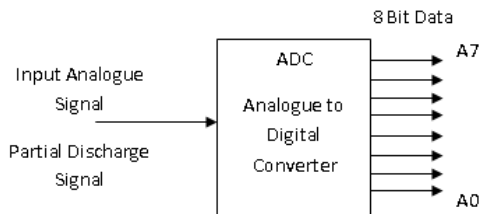


Fig. 4 Block Diagram Data ADC

Fig. 5 shows the output data in ADC block. There are 256 levels to convert Analogue Data to Digital Data when process conversion data from 0 Volt to 5 Volt.

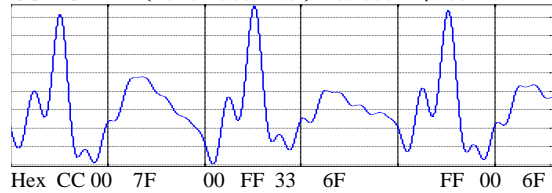
OUTPUT Data in ADC Block:

A7 A6 A5 A4 A3 A2 A1 A0
 (5 Volt) FF = 1 1 1 1 1 1 1 1

 (0 Volt) FF = 0 0 0 0 0 0 0 0

Fig. 5 Output Data in ADC Block

A.2. Process Convert PD Signal Data in ADC:



Data Convert: 1 Volt = 33 hex 2 Volt = 66 hex
 3 Volt = 99 hex 4 Volt = CC hex 5 Volt = FF hex.

Fig. 6 Output Data of ADC Block in Hexadecimal

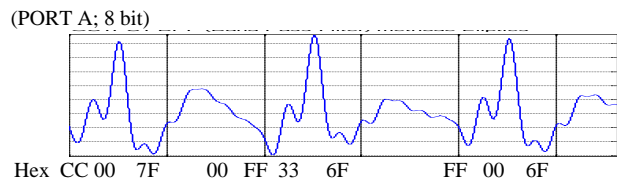
Equation:

$$X \text{ Volt} = \frac{x \cdot 255}{5} \text{ dec} = \text{convert to hex} \dots (1)$$

A.3. Data input Partial Discharge in Binary Data:

OUTPUT ADC (bin):

Fig. 7 shows the output data of ADC block in binary digital.



Bin:

A ₇	1	0	0	0	1	0	0	1	0	0
A ₆	1	0	1	0	1	0	1	1	0	1
A ₅	0	0	1	0	1	1	1	1	0	1

A ₄	0	0	1	0	1	1	0	1	0	0
A ₃	1	0	1	0	1	0	1	1	0	1
A ₂	1	0	1	0	1	0	1	1	0	1
A ₁	0	0	1	0	1	1	1	1	0	1
A ₀	0	0	1	0	1	1	1	1	0	1

Fig. 7 Output Data of ADC Block in Binary digital

A.4. Design ADC and PEAK Detection in FPGA:

The function of this peak detector is for detect peak signals PD from sensor. In this simulation the peak detector is designed to have a 2.8 V = 8F hex threshold voltage. It means that if the input signal is more than 2.8 V or 8F hex, the output of the peak detector is logic 1 or 5 V and if input signal is less than 2.8 V or 8F hex, the output peak detector is logic 0 or 0 V. Detail of simulation model of Peak detector is shown in Fig.8.

A.5. Block Diagram Simulation Model FPGA for ADC and PEAK Detection:

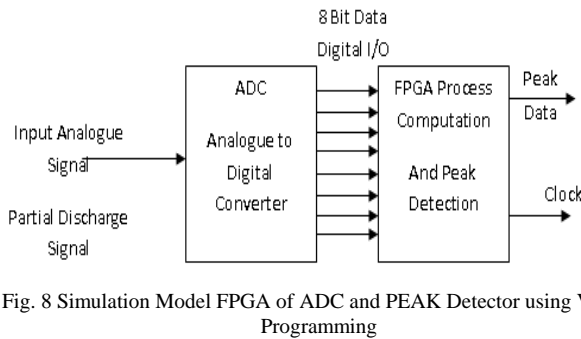


Fig. 8 Simulation Model FPGA of ADC and PEAK Detector using VHDL Programming

Comparator :

(Threshold = 8F hex = 2.803 Volt)

Threshold is designed in value 2.803 Volt or 8F hex to detect PD signals in peak detector block. Output of peak detector is logic high (logic 1=5V), if the input peak detector block is more than 8F hex or if input ADC block is more than 2.803 Volt. Output of peak detector is logic low (logic 0=0V), if the input peak detector block is less than 8F hex or if input ADC block is less than 2.803 Volt.

A.6. Design Threshold for ADC and Peak Detector Block:

Design Threshold for Analogue Signal of Input Partial Discharge Signal:

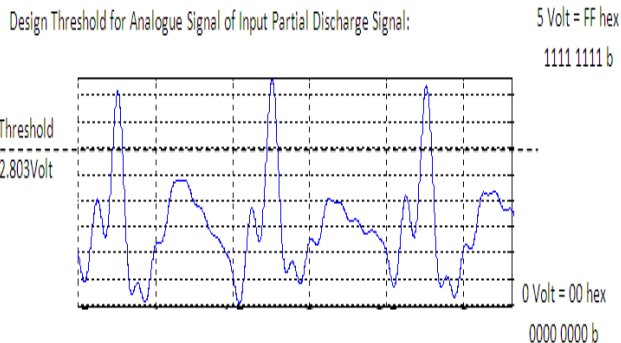


Fig. 9 Design Threshold for Input Data Analogue from ADC

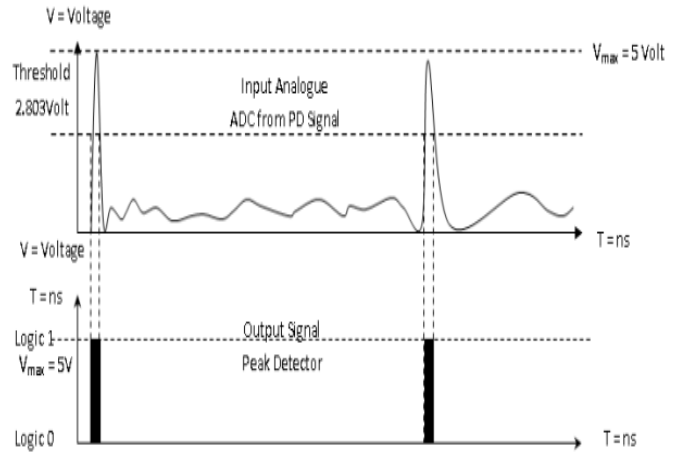


Fig. 10. Design Threshold and Process Peak Detection

Fig. 9 shows the design threshold for input data analogue of ADC block in peak detector. Fig.10. shows the design threshold and output data of peak detector.

A.7. Comparator between design VHDL and Verilog Programming for ADC and PEAK Detection block in FPGA:

A.7.1. VHDL Programming:

```

library IEEE;
use IEEE.STD_LOGIC_1164.ALL;
use IEEE.STD_LOGIC_ARITH.ALL;
use IEEE.STD_LOGIC_UNSIGNED.ALL;

entity ADCandPEAK is
Port ( CLOCK : in STD_LOGIC;
      ADC : in STD_LOGIC_VECTOR (7 downto 0);
      PEAK : out STD_LOGIC);
end ADCandPEAK;
```

```

architecture Behavioral of ADCandPEAK is
signal PEAK_DETECT : std_logic := '0';
begin

process (CLOCK)
begin

if (CLOCK'event and CLOCK = '1') then
if (ADC > "10001111") then
PEAK_DETECT <= '1';
else
PEAK_DETECT <= '0';
end if;
end if;
end process;
PEAK <= PEAK_DETECT;
end Behavioral;
```

A.7.2. Verilog Programming

```

module ADCandPEAK(CLOCK, ADC, PEAK);
input CLOCK;
input [7:0] ADC;
output PEAK;

reg [0:0] PEAK = 1'b0;
reg [7:0] threshold = 8'h8F; //or threshold = 8'b1000_1111;

always @(posedge CLOCK)
if (ADC > threshold)
```

```

PEAK <= 1'b1;
else
PEAK <= 1'b0;

```

Endmodule

Listing programming A.71 shows the design VHDL programming for ADC and Peak detector block in FPGA technology. Listing programming A.72 shows the design Verilog programming for ADC and Peak detector block inn FPGA technology.

A.8. Flow Chart Diagram for ADC and PEAK Detection Programming:

Fig.10. shows the design flowchart diagram.

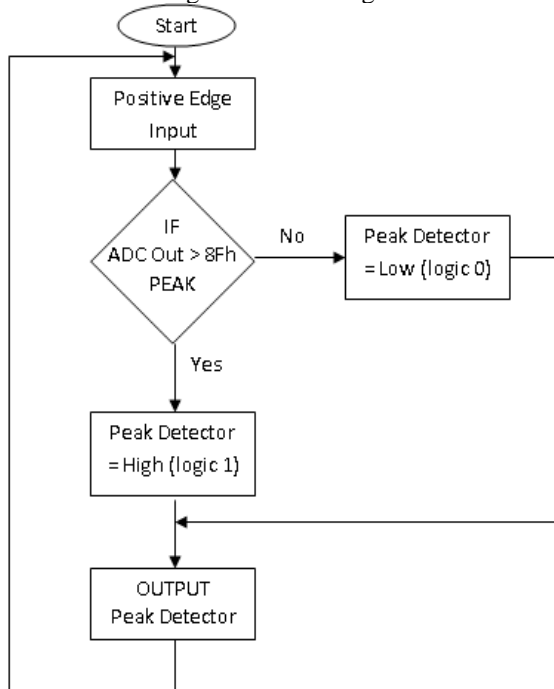


Fig.11. Design Flow Chart Diagram for ADC and Peak Detection Block in FPGA

Fig. 11 shows the design flow chart diagram for ADC and peak detector block in FPGA.

A.9. Design Input Data Analogue ADC for Simulation PD signal in ADC and PEAK Detector of FPGA:

Fig.12 shows the design input PD signal to FPGA board from ADC board before simulation VHDL using Xilinx ISE simulator.

Design input data before simulation as follow:

1. Input data 1st impulse from ADC is: 1110 1111 or EF hex (4.686 V).
2. Input data 2nd impulse from ADC is: 0000 0000 or 00 hex (0 V).
3. Input data 3rd impulse from ADC is: 1101 1111 or DF hex (4.372 V)
4. Input data 4th impulse from ADC is: 1011 1111 or BF hex (3.745 V)

5. Input data 5th impulse from ADC is: 0010 0000 or 20 hex (0.62 V).
6. Input data 6th impulse from ADC is: 0000 1000 or 08 hex (0.157 V).
7. Input data 7th impulse from ADC is: 0000 0010 or 02 hex (0.039 V).

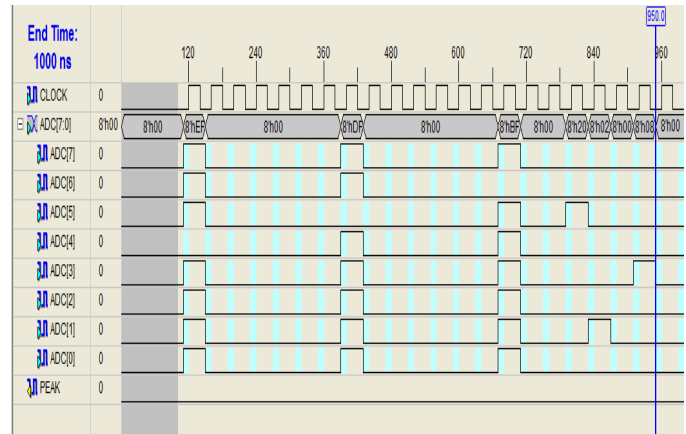


Fig.12. Design Input Data Analogue PD signal for ADC and Peak Detection Block

A.10. Design Platform FPGA for ADC and PEAK Detector Block:

Platform programming is VHDL (Very high speed integrated circuit Hardware Description Language) and Verilog programming.

Platform FPGA is:

1. FPGA Virtex 5 (ML501 Board)
2. Chipset FPGA is XC5VLX50
3. Package of Chipset is FF676

Design clock timing in FPGA Xilinx Virtex 5 is:

1. Clock High Time is : 20 ns
2. Clock Low Time is : 20 ns
3. Input setup Time is : 10 ns
4. Output Valid Delay is : 10 ns
5. Offset is : 100 ns
6. Initial Length of Test Bench is : 1000 ns

A.11. Result Test Simulation for ADC and Peak Detector Block Programming:

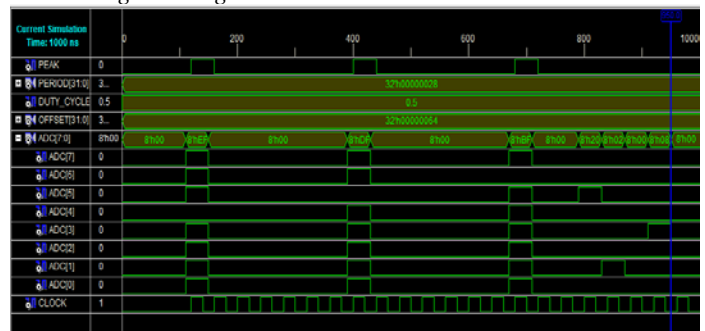


Fig.13. Simulation Model FPGA of ADC and Peak Detector Block using Test Bench Wave ISE Simulator from 0 ns until1000 ns

A.11.1 Analysis Graphic:

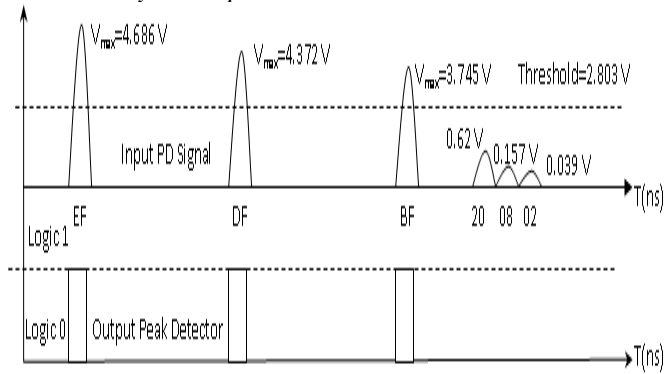


Fig.14. Analysis Simulation Model FPGA of ADC and Peak Detector Block Programming.

Result Test in fig.13. shows the peak detector can detect Peak of PD signal from input signal ADC. The Peak detector in this simulation is designed to have a 2.803 V = 8F hex threshold voltage. It means that if the input signal is more than 2.803 V or 8F hex, the output of the peak detector is logic 1 or 5 V and if input signal is less than 2.803 V or 8F hex, the output peak detector is logic 0 or 0 V. Detail of simulation model result of Peak detector is shown in Fig.14.

A.11.2 Conclusion of the Simulation:

This ADC and PEAK Detection Block has been successful to be running in FPGA Programming.

B. Block Counter and Reset :

B.1. Design Counter and Reset Block:

The purpose of the Counter and Reset Block is for counting the amount of PD signals from ADC signal and Peak detection Block in the FPGA and then perform the computation of the real time data using 30 bit digital Output data in VHDL Programming. So it means counter will run up counter from 0 to 1,073,741,824 counting or 0000 0000 hex to 3FFF FFFF hex counting. Counter will return back to 0 if the reset of counter is active. In this VHDL programming, counter is designed using reset active high (type negative edge reset) for Up Counter in FPGA. Fig.15. shows the input data analogue from ADC.

Digital Signal of Input Counter and Reset Block in FPGA:

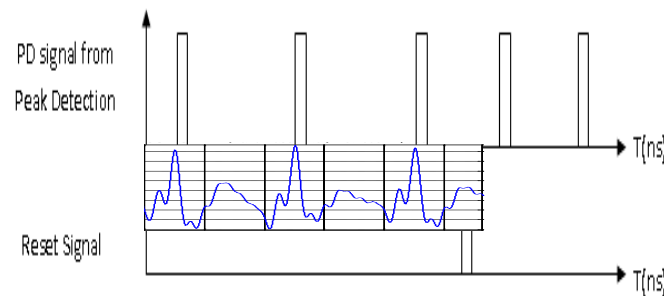


Fig.15. Input Data Analogue from ADC

B.2. Block Diagram:

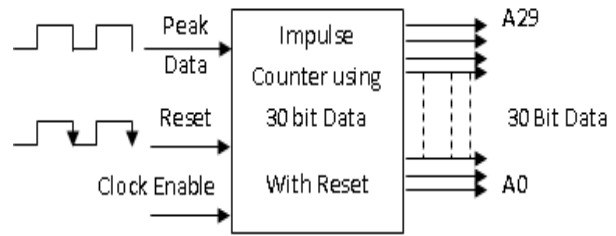


Fig.16. Block Diagram Design for 30 bit Counter and Reset Block in FPGA

Fig.16. shows the design 30 bit up counter with reset in FPGA.

OUTPUT Data in Counter and Reset Block:

```

A29 A28 A27..... A3 A2 A1 A0
3FFF FFFF = 1 1 1 ..... 1 1 1 1
-----
0000 0000 = 0 0 0 ..... 0 0 0 0
    
```

There are 1,073,741,824 levels counting to count Digital PD signal Data from Peak detector when process counting data from 0000 0000 hex to 3FFF FFFF hex.

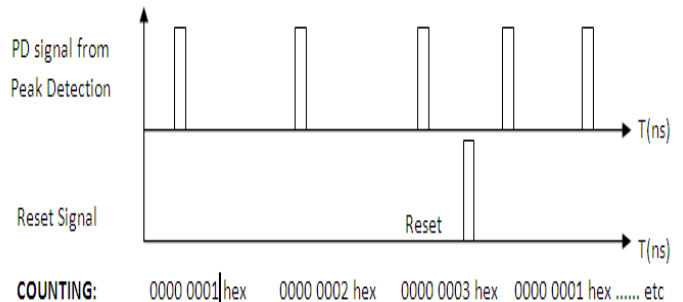


Fig.17. Block Diagram Design for 30 bit Counter and Reset Block in FPGA

Fig.17 shows desire result from design counter with reset block programming. The desire result have to show the output up counter increase when there is impulse signal, and the output up counter must be zero when the reset signal is active.

B.3. Flow Chart Diagram for Counter and Reset Block Programming:

Fig.18. shows the design flowchart diagram of Counter and Reset Block in FPGA. The first time program of counter is setting to positive edge input. The second step of the program is select data input, if the input reset data is active or logic high then the output counter must be reset to zero value. If the input reset data is not active or logic low, the program will continue the next step. The third step of the program is select input data of CE (chip enable). If the CE is given data active or logic high then the output data counter must be increase data by 1. If the CE is not active then data output counter must be the same with old data. So data output counter will be stop if CE is not active and the counter will run again after the input CE is active again.

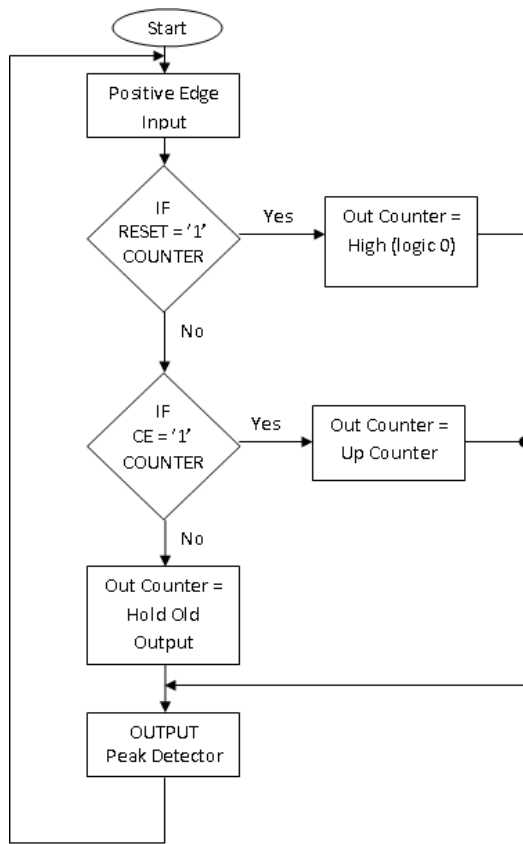


Fig.18. Design Flow Chart Diagram for Counter and Reset Block in FPGA

B.4. Result Test Simulation for Counter and Reset Block Programming:

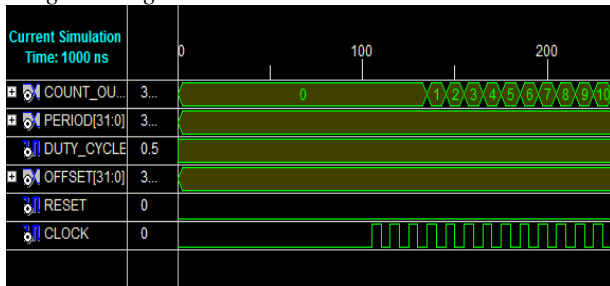


Fig.19. Simulation Model FPGA of Counter and Reset Block using Test Bench Wave ISE Simulator from 0 ns until 230 ns

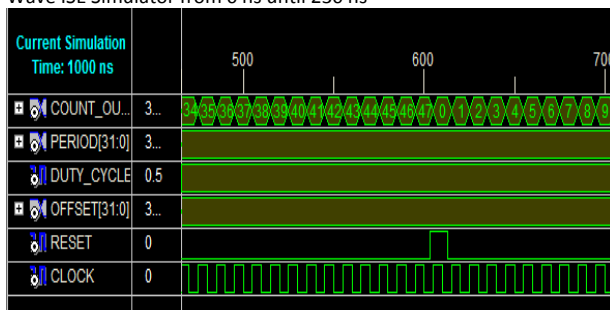


Fig.20. Simulation Model FPGA of Counter and Reset Block using Test Bench Wave ISE Simulator from 500 ns until 700 ns

B.4.1. Analysis Graphic:

Fig.20 and 21 shows the up counter is running from 0 to 46 hex when Reset is not active and Chip Enable is active. Up

counter is running depend of amount impulse Peak Detector from input Counter and Reset Block. If there is impulse reset is active in 600 ns, the counter is return back to 0 and do up counting again.

B.4.2. Conclusion of the Simulation:

The Up Counter and Reset Block has been successful to synthesis, compile, simulate and run in FPGA Programming.

C. Combination ADC-Peak Detection and Counter-Reset Block

C.1. Design Peak Detector and Up Counter Block:

The counter will reset each 1µs, and the data output will be hold by a latch for display purpose. The data will be updated to display each 0.5µs or 500ns in FPGA. For constant impulse signal rate, there will be 10⁸ Impulse in 1 second if there is 1 impulse in each 10 ns. In real system data will be updated to display each 1second in FPGA.

C.2. Block Diagram of Peak Detector and Counter:

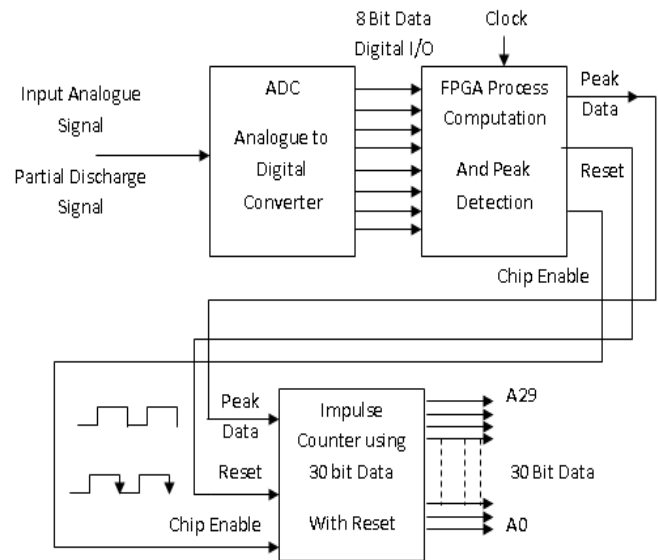


Fig.21. Simulation Model FPGA of Peak Detector and Up Counter Block using Test Bench Wave ISE Simulator

Fig.21. shows the simulation model FPGA of peak detector and up counter with reset block.

Design clock timing in FPGA Xilinx Virtex 5 for simulation model FPGA of peak detector and up counter with reset block is:

1. Clock High Time is : 5 ns
2. Clock Low Time is : 5 ns
3. Input setup Time is : 2 ns
4. Output Valid Delay is : 2 ns
5. Offset is : 100 ns
6. Initial Length of Test Bench is : 1000 ns

C.3. Flow Chart Diagram for Combination ADC with Peak Detector Block and Counter with Reset Block Programming:

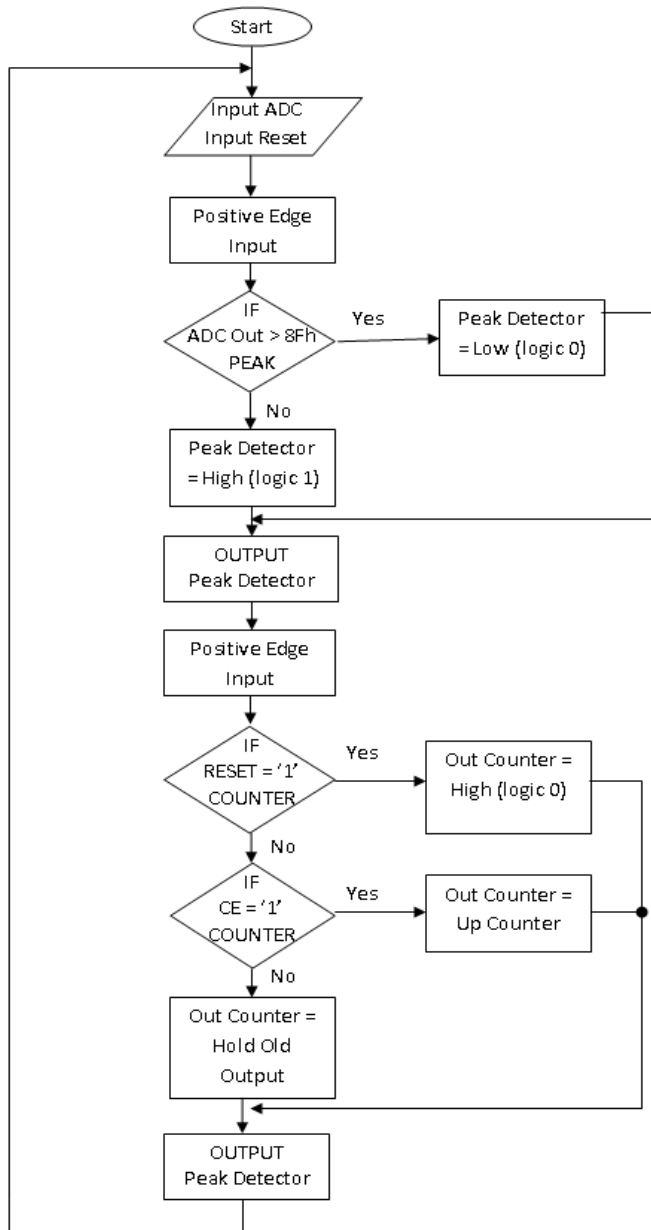


Fig.22.Simulation Combination Peak Detector Block and Counter Block

Fig.22. shows the design flowchart diagram of Combination ADC with Peak Detector Block and Counter with Reset Block in FPGA.

III. SIMULATION RESULT

A.Test Simulation FPGA using Test Bench Wave for ADC and PEAK Detection Programming:

A.1. Simulation Result Graph:

Fig. 23 shows the result test simulation model of ADC and Peak Detector block programming. Table.1 shows the data result of simulation test of ADC and Peak Detector block programming. Fig.24 shows the analysis graphic of simulation ADC and Peak Detector block programming.

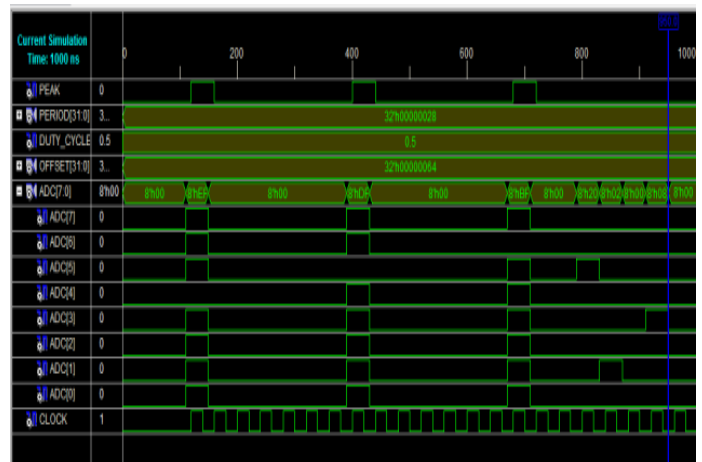


Fig.23. Simulation Model FPGA of ADC and PEAK Detector using Test Bench Wave ISE Simulator

A.2. Result Test:

Table 1. Data Result Test Peak Detector

Input Data From ADC		Threshold = 8F hex = 2.803 Volt		
No.	Data Binary	Data Hex	Data in Voltage	Output Peak
01.	1110 1111	EF	4.686 V	high (logic 1)
02.	0000 0000	00	0 V	low (logic 0)
03.	1101 1111	DF	4.372 V	high (logic 1)
04.	1011 1111	BF	3.745 V	high (logic 1)
05.	0010 0000	20	0.62 V	low (logic 0)
06.	0000 1000	08	0.157 V	low (logic 0)
07.	0000 0010	02	0.039 V	low (logic 0)

The data experiment lab of simulation VHDL programming shows output peak detection is logic high when the input voltage more than 2.803 volt.

A.3. Analysis Graphic:

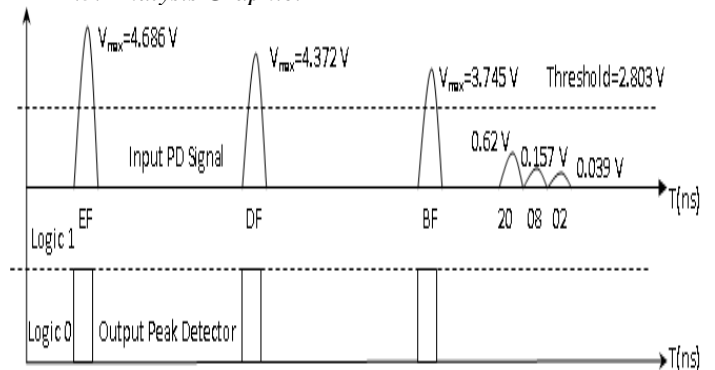


Fig.24. Analysis Graphic of Simulation Model FPGA for ADC and PEAK Detector Block

B.Simulation FPGA for Combination ADC with Peak Detector Block and Counter with Reset Block Programming

B.1. Simulation Result:

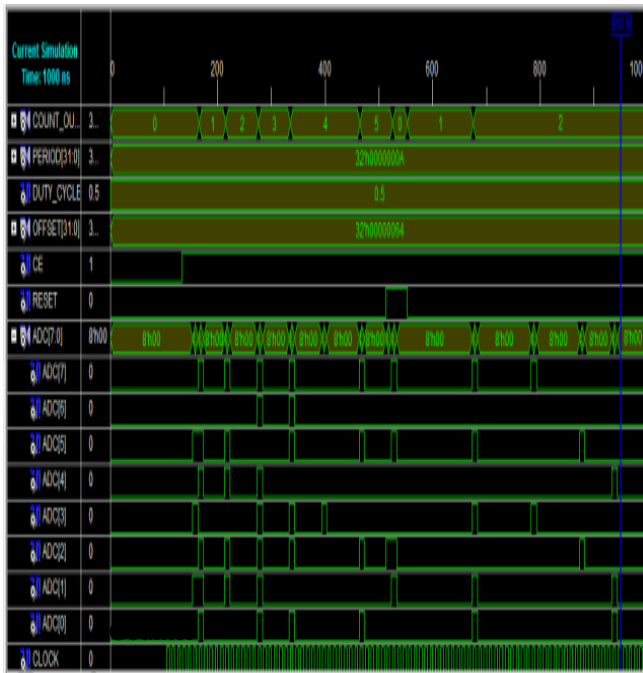


Fig.25. Test Simulation FPGA for Peak Detector and Up Counter Block using Test Bench Wave

B.2. Analysis Graphic:

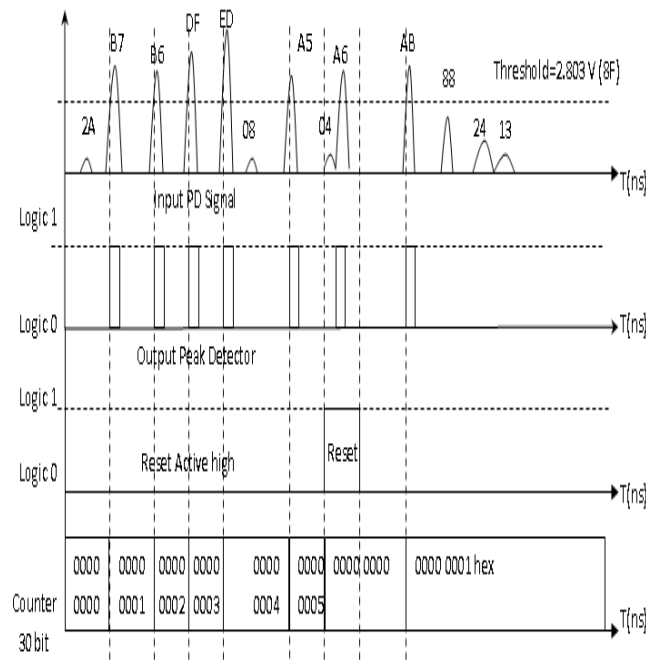


Fig.26. Analysis Graphic Signal for Peak Detector and Up Counter Block in Simulation FPGA

Fig.25 shows the result test of simulation combination ADC with peak detector block and counter with reset block programming in VHDL. Fig.26 shows the analysis graphic signal of combination ADC with peak detector block and counter with reset block. Fig.25 and 26 shows the up counter is running from 0 to 5 hex when Reset is not active and Chip Enable is active. Up counter is running depend of amount impulse Peak Detector from input Counter and Reset Block. If

there is impulse reset is active in 500 ns, the counter is return back to 0 and do up counting again.

The up counter is counting when there is input analogue PD signal from ADC that more than threshold line 2.803 Volt or 8F hex. The up counter will return to zero (0) again if reset is active (the reset is active high).

V. CONCLUSSION

Result Test show that Output Peak Detector can detect Peak signal from input signal ADC. The Peak detector in this simulation is designed to have a 2.803 V = 8F hex threshold voltage. It means that if the input signal is more than 2.803 V or 8F hex, the output of the peak detector is logic 1 or 5 V and if input signal is less than 2.803 V or 8F hex, the output peak detector is logic 0 or 0 V. This ADC and PEAK Detection Block has been successful to be running in FPGA Programming.

The ADC-Peak Detector and Up Counter-Reset Block has been successful to synthesis, compile, simulate and run in FPGA Programming. Combination ADC-Peak-Counter can work successfully.

VII. REFERENCE

- [1] Ahmad Basri bin Abdul Ghani, "Detection of Partial Discharge in Underground Cable Using Magnetic Probe," in 2008 Doctoral Thesis in University Tenaga Nasional, Malaysia, 2008.
- [2] A. Morgado, V.J. Rivas, R. del Rio, R. Castro-Lopez, F. Fernandez and J.M de la Rosa, "Behavioral Modeling, Simulation and Synthesis of Multi-standard Wireless Receivers in MATLAB/SIMULINK" VLSI Journal 2008, Vol.41.
- [3] Bill Schwartz, Michael Carfore, and Dr. Robert Qiu, "Ultra Wideband Transmitter & Receiver Design," in The REU Program of Tennessee Technological University, July 27, 2005.
- [4] Benjamin Nicolle, Mourad Zarour, William Tatinian, Gilles Jacquemod, "System Design Oriented Low Noise Amplifier Modeling" in IEEE 2007
- [5] S. Braun, F. Krug, and P. Russer, "A novel automatic digital quasi-peak 60detector for a time domain measurement system," in 2004 IEEE International Symposium On Electromagnetic Compatibility Digest, August 9-14, Santa Clara, USA, 2004.
- [6] CISPR16-1, Specification for radio disturbance and immunity measuring apparatus and methods Part 1: Radio disturbance and immunity measuring apparatus. International Electrotechnical ommission, 1999.
- [7] L. Cohen, "Time-Frequency Distributions - A Review," in Proceeding of the IEEE, vol. 77, no. 7, pp. 941-981, 1989.[4] A. V. Oppenheim and R. W. Schafer, Discrete-Time Signal Processing. ISBN 0-13-214107-8, Prentice-Hall, 1999.
- [8] M. S. Chong, "Partial Discharge Mapping of Medium Voltage Cables - TNB's Experience", CIRED 2001, 18-21 June 2001, Conference Publication No. 482 © IEEE 2001
- [9] F.H Kreuger, "Discharge Detection in High Voltage Equipment", A Heywood Book, Temple Press Book Ltd, London 1964.
- [10] Xilinx Tutorial Documentation, "ISE 9.1i Quick Start Tutorial", Copyright © Xilinx, Inc. All rights reserved, 1995-2007.

**Emilliano**

S.Pd First degree in Electrical and Electronics (University Negeri Jakarta, Indonesia), 2001
 M.T. Master Engineering in Department of Electrical Engineering in Control Engineering LSKK-EE-ITB (Bandung Institute of Technology, ITB), 2005
 E-Mail: emilliano@uniten.edu.my
 Telephone: +60 3 89212020 ext. 3288
 Office: BW-4R-015

Area of Research:

Automatic Real Time System of Partial Discharge Detection for Under Ground Cable Using Giga Hertz Speed Data Acquisition and Xilinx FPGA Technology in VHDL Programming.

**Assoc. Prof. Dr. Chandan Kumar Chakrabarty MIMM, InstP, CPhys, CEng**

Ph. D. (RF Plasma Technology) (Flinders Univ., Australia), 1996
 M.Sc. (Pulsed Plasma Technology) (Univ. of Malaya, Malaysia), 1988
 B. Sc. (Hons.) in Physics (Univ. of Malaya, Malaysia), 1986.
 E-Mail: chandan@uniten.edu.my

Telephone: +60 3 8921 3230

Office: BW-2-C030

Area of Specialization / Research Interest:

Radio Frequency and Microwave Technology, Gas Discharge Physics

**Dr Agileswari K. Ramasamy**

Ph. D. in Electrical Engineering (Univ. Tenaga Nasional, Malaysia)
 M. Sc. in Control Systems (Imperial College, UK)
 B. Sc. in Electrical Engineering (Purdue Univ., USA)
 E-Mail: agileswari
 Telephone: +60 3 8921 2270
 Office: BN-1-031

**Dr . Ir. Ahmad Basri bin Abdul Ghani**

TNB Research Sdn. Bhd. As the Technical Manager for High Voltage Testing Laboratory.
 PhD in Electrical Engineering with split PhD program between Univ. Tenaga Nasional, Malaysia and University of Southampton, UK.
 Master in Engineering Management at Univ. Tenaga Nasional, Malaysia.

B.Eng. (Hons) in Electrical Engineering at University of Southampton, UK.

E-Mail: abasri.aghani@tnbr.com.my

Note: An earlier version of this paper was presented at the ICA2009 International Conference in October 2009 in Bandung, Indonesia.

Internetworking Indonesia Journal

The Indonesian Journal of ICT and Internet Development
ISSN: 1942-9703

About the Internetworking Indonesia Journal

The Internetworking Indonesia Journal (IJ) was established out of the need to address the lack of an Indonesia-wide independent academic and professional journal covering the broad area of Information and Communication Technology (ICT) and Internet development in Indonesia.

The broad aims of the Internetworking Indonesia Journal (IJ) are therefore as follows:

- **Provide an Indonesia-wide independent journal on ICT:** The IJ seeks to be an Indonesia-wide journal independent from any specific institutions in Indonesia (such as universities and government bodies). Currently in Indonesia there are numerous university-issued journals that publish papers only from the respective universities. Often these university journals experience difficulty in maintaining sustainability due to the limited number of internally authored papers. Additionally, most of these university-issued journals do not have an independent review and advisory board, and most do not have referees and reviewers from the international community.
- **Provide a publishing venue for graduate students:** The IJ seeks also to be a publishing venue for graduate students (such as Masters/S2 and PhD/S3 students) as well as working academics in the broad field of ICT. This includes graduate students from Indonesian universities and those studying abroad. The IJ provides an avenue for these students to publish their papers to a journal which is international in its reviewer scope and in its advisory board.
- **Improve the quality of research & publications on ICT in Indonesia:** One of the long term goals of the IJ is to promote research on ICT and Internet development in Indonesia, and over time to improve the quality of academic and technical publications from the Indonesian ICT community. Additionally, the IJ seeks to be the main publication venue for various authors worldwide whose interest include Indonesia and its growing area of information and communication technology.
- **Provide access to academics and professionals overseas:** The Editorial Advisory Board (EAB) of the IJ is intentionally composed of international academics and professionals, as well as those from Indonesia. The aim here is to provide Indonesian authors with access to international academics and professionals who are aware of and sensitive to the issues facing a developing nation. Similarly, the IJ seeks to provide readers worldwide with easy access to information regarding ICT and Internet development in Indonesia.
- **Promote the culture of writing and authorship:** The IJ seeks to promote the culture of writing and of excellent authorship in Indonesia within the broad area of ICT. It is for this reason that the IJ is bilingual in that it accepts and publishes papers in English and Bahasa Indonesia. Furthermore, the availability of an Indonesia-wide journal with an international advisory board may provide an incentive for young academics, students and professionals in Indonesia to develop writing skills appropriate for a journal. It is hoped that this in-turn may encourage them to subsequently publish in other international journals in the future.

Focus & Scope: The Internetworking Indonesia Journal (IJ) aims to become the foremost publication for practitioners, teachers, researchers and policy makers to share their knowledge and experience in the design, development, implementation, and the management of ICT and the Internet in Indonesia.

Topics of Interest: The journal welcomes and strongly encourages submissions based on interdisciplinary approaches focusing on ICT & Internet development and its related aspects in the Indonesian context. These include (but not limited to) information technology, communications technology, computer sciences, electrical engineering, and the broader social studies regarding ICT and Internet development in Indonesia. A list of topics can be found on the journal website at www.InternetworkingIndonesia.org.

Open Access Publication Policy: The Internetworking Indonesia Journal provides open access to all of its content on the principle that making research freely available to the public supports a greater global exchange of knowledge. This follows the philosophy of the Open Journal Systems (see the Public Knowledge Project at pkp.sfu.ca). The journal is published electronically (PDF format) and there are no subscription fees. Such access is associated with increased readership and increased citation of an author's work.

Internetworking Indonesia Journal

ISSN: 1942-9703

www.InternetworkingIndonesia.org